

**EFFECT OF SHEAR DEFORMATION ON STATIC AND  
DYNAMIC BEHAVIOR OF THICK FUNCTIONALLY  
GRADED MATERIAL PANELS**

BY

**Sultan Mohammedali A. Ghazzawi**

A Thesis Presented to the  
DEANSHIP OF GRADUATE STUDIES

**KING FAHD UNIVERSITY OF PETROLEUM & MINERALS**  
DHAHRAN, SAUDI ARABIA

In Partial Fulfillment of the  
Requirements for the Degree of

**MASTER OF SCIENCE**

In  
**AEROSPACE ENGINEERING**

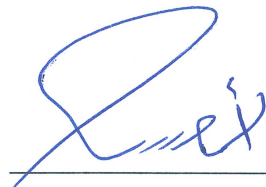
**December 2018**

KING FAHD UNIVERSITY OF PETROLEUM & MINERALS

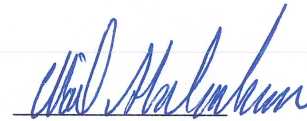
DHAHRAN- 31261, SAUDI ARABIA

**DEANSHIP OF GRADUATE STUDIES**

This thesis, written by **Sultan Mohammedali A. Ghazzawi** under the direction of his thesis advisor and approved by his thesis committee, has been presented and accepted by the Dean of Graduate Studies, in partial fulfillment of the requirements for the degree of **MASTER OF SCIENCE IN AEROSPACE ENGINEERING**



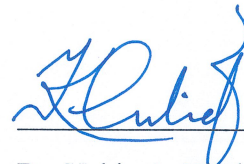
Dr. Ayman M. Abdallah  
Department Chairman



Dr. Wael G Abdelrahman  
(Advisor)




Dr. Salam A. Zummo  
Dean of Graduate Studies



Dr. Yehia A. Khulief  
(Member)

25/12/2018

Date



Dr. Ayman M. Abdallah  
(Member)

© Sultan Mohammedali A. Ghazzawi

2018

*Dedicated to my lovely mother,  
father and wife*

# ACKNOWLEDGMENTS

IN THE NAME OF ALLAH, THE MOST BENEFICENT, THE MOST  
MERCIFUL

*“And they ask you, [O Muhammad], about the soul. Say, the soul is of the affair of my Lord. And mankind has not been given of knowledge except a little.”*

(The Holly Quran, Surah No. 85)

Thanks to Allah for giving me all the uncountable blessings that I have in my life, and for giving the opportunity to contribute toward the overall knowledge of humanity.

Great thanks to His Majesty The Custodian of The Two Holy Mosques, HRH The Crown Prince, as one of Saudi youths for facilitating and giving us the opportunity to seek knowledge from higher education institutions. Thanks to King Fahd University of Petroleum and Minerals, for taking care of me since the start of my BS in 2010, giving me the opportunity to continue my MS degree in the aerospace department and being a member of KFUPM innovative family as a graduate assistant. It is my honor to be involved in such a great university. All my love and loyalty to my country, my university and my department.

This work would never be accomplished without the help, support and mentoring of my advisor **Dr. Wael G Abdulrahman**. His continuous support and dedication were my thrust throughout my research time and study. His support goes back to my BS days, I did not forget his encouragements during the time when I studied several aerospace courses with him. Then when he became my coop advisor, I had the opportunity to work under his

mentorship, where he continually supported me to do my best. I cannot thank him enough for his help!

My gratitude and thanks for **Dr. Ayman Abdallah**, Chairman of Aerospace Department and a member in my thesis committee, for his kindness, patience, soft support throughout my MS study. He was more like an older brother to me, he educated, advised and guided me throughout my research and study, while pushing me gently to perform my work in the best way I can. That was one of my challenging time, and I appreciate him so much. May Allah bless him and his family.

I would acknowledge **Dr. Yehia A. Khulief** for participating and sharing his valuable experience and knowledge for helping me accomplish my thesis. His overall supervision and guidance were fruitful for me.

Thanks to all AE faculty members, particularly Dr. Ahmed Al-Garni, since he was eager to motivate me for doing my higher education and being involved in AE department as a future faculty. Moreover, special thanks to all AE staffs, along with my supportive colleagues, namely Mr. Mohammed A. Muqeeth and Mr. Hamza Mir for helping me in proofreading work. Special thanks also to Mr. Muhydeen Olorunlana, for his great help during my literature review work.

I am so thankful to my beloved mother, Fayruz Talib, who never stopped praying for me and supporting me from all aspects. She took care of me and raised me alone. She was my first great motivation to be a researcher. This work is dedicated to her! All thankful words would never be enough to say thanks for my father, Mohammedali A Ghazzawi, although he died, when I was a child, I still feel his support and motivation throughout my

entire life. I will remember him and pray for him as long as I live. Thanks to my lovely sister Mrs. Fatin Ghazzawi. I would never forget her help and emotional support. I would like also to appreciate my friends' help and encouragement, namely Mr. Muayed Wali, Mr. Hamzah Gazzaz and Mr. Abdullah Hakami for being careful and supportive friends. I am thankful and grateful to have you as friends.

All my thanks and appreciations are also dedicated to my beloved wife, Shrooq Bukhari. She is my great factor of success, with being emotionally supportive, she tirelessly took care of me, like a mother to her child. I was able to perform well during my study and research time because of her tenderness.

Finally, I hope this work would be beneficial to someone, somewhere in the world. I also hope that it would be just a beginning of more fruitful and innovative research works for the sake of humanity's knowledge.

# TABLE OF CONTENTS

<b>ACKNOWLEDGMENTS</b> .....	<b>v</b>
<b>TABLE OF CONTENTS</b> .....	<b>viii</b>
<b>LIST OF TABLES</b> .....	<b>x</b>
<b>LIST OF FIGURES</b> .....	<b>xi</b>
<b>LIST OF ABBREVIATIONS</b> .....	<b>xiv</b>
<b>ABSTRACT</b> .....	<b>xv</b>
<i>ملخص الرسالة</i> .....	<b>xvii</b>
<b>CHAPTER 1 INTRODUCTION</b> .....	<b>1</b>
1.1 Composites and Laminated Composite .....	1
1.2 Functionally Graded Materials.....	3
1.3 Classification of FGM Plates.....	6
<b>CHAPTER 2 LITERATURE REVIEW</b> .....	<b>10</b>
2.1 Research on Static and Dynamic Response of FGM Structures.....	10
2.2 Research of FGM Plates Responses Using CPT .....	14
2.3 Research of FGM Plate Response using FSDT.....	16
2.4 Research of FGM Plate Response using HSDT .....	18
2.5 Motivation and Objective .....	25
2.6 Thesis Organization.....	26
<b>CHAPTER 3 MATHEMATICAL FORMULATION OF FGM PANELS</b> .....	<b>28</b>
3.1 Kinematics of Different Plate Theories .....	28
3.2 General Assumptions and Configuration.....	33
3.3 Classical Plate Theory (CPT) .....	36
3.3.1 Governing Equation .....	36
3.3.2 Series Solution of CPT .....	38
3.4 Third Order Shear Deformation Theory (TSDT) .....	42
3.4.1 Governing Equations.....	42
3.4.2 Series Solutions (The Navier's Solutions).....	45
<b>CHAPTER 4 NUMERICAL RESULTS AND DISCUSSIONS</b> .....	<b>49</b>



4.1	Validation of The Model .....	49
4.1.1	Validating Model of Static Responses.....	50
4.1.2	Validating Model of Dynamic Responses .....	51
4.2	Parametric Study.....	54
4.2.1	Static Responses of Classes of FGM Panels .....	54
4.2.2	Dynamic Responses of Classes of FGM.....	64
<b>CHAPTER 5</b>	<b>EFFECTS OF SHEAR DEFORMATION .....</b>	<b>72</b>
5.1	Shear Effects on Maximum Deflection .....	73
5.2	Shear Effects on Fundamental Natural Frequency .....	82
<b>CHAPTER 6</b>	<b>CONCLUSIONS.....</b>	<b>84</b>
6.1	Summary .....	84
6.2.	Aspects for Improvements in Future Work .....	86
<b>REFERENCES</b>	<b>.....</b>	<b>87</b>
<b>VITAE</b>	<b>.....</b>	<b>93</b>

## LIST OF TABLES

Table 1:	Widely used types of FGM and their applications [1].....	6
Table 2:	FGM plate Material properties.....	49
Table 3:	Comparing Dimensionless Deflections between the present model and Mechab et al. [28] model for a P-FGM plate.....	51
Table 4:	Comparative study between the present TSDT, Model II for Mechab et al. [28] and HSDT, for fundamental frequencies parameters of a P-FGM square plate.....	53
Table 5:	Material properties of several combinations of the constituents of a ceramic- metal FGM panels.....	67
Table 6:	Dimensionless Maximum Deflections of P-FGM and S-FGM square plates with various power indices and thickness ratios obtained by CPT and TSDT.. .....	78
Table 7:	Dimensionless Maximum Deflections of E-FGM square plates with various power indices and thickness ratios obtained by CPT and TSDT.....	79
Table 8:	Effect of Shear deformation on the non-dimensional fundamental frequencies refer to the first three modes of P-FGM .....	83

## LIST OF FIGURES

Figure 1:	A house made of wattle and doub.....	2
Figure 2:	Laminated composite specimen.....	3
Figure 3:	Concept of composition graduation in composites [1] .....	4
Figure 4:	Effect of Power Law on Young’s modulus Across the Plate Thickness [2]...	7
Figure 5:	Effect of Sigmoid Law on Young’s Modulus Across the Plate Thickness [2]. .....	8
Figure 6:	Effect of Exponential Law on Young’s Modulus Across the Plate Thickness [2].....	9
Figure 7:	The coordinate system of a rectangular plate [31].....	29
Figure 8:	Concept of the deformation of a transverse normal for the elastic plate theories [31] .....	29
Figure 9:	FGM plate geometric features .....	34
Figure 10:	A small element of the plate subjected to forces and moments [2] .....	36
Figure 11:	Effects of varying power indices and thickness ratios on the plate’s maximum deflection on P-FGM and S-FGM .....	55
Figure 12:	Effects of varying power indices and aspect ratios on the plate’s maximum deflection on P-FGM and S-FGM .....	57
Figure 13:	Effects of varying Young’s modulus ratios and thickness ratios on the plate’s maximum deflection for a) P-FGM, b) S-FGM, and c) E-FGM, from top left to bottom, respectively.....	59

Figure 14: Effects of varying Young’s modulus ratios and aspect ratios on the plate’s maximum deflection for P-a) FGM, b) S-FGM, and c) E-FGM from top left to bottom, respectively..... 60

Figure 15: Comparing the effects of varying Young’s modulus ratios and thickness ratios on the plate’s maximum deflection between P-FGM, S-FGM and E-FGM..... 61

Figure 16: Comparing the effects of varying Young’s modulus ratios and aspect ratios on the plate’s maximum deflection between P-FGM, S-FGM and E-FGM..... 62

Figure 17: Differences between classes of FGM plates in terms of the maximum deflection vs. thickness ratios when subjected to a point load and a sinusoidal distributed load ..... 63

Figure 18: Differences between classes of FGM plates in terms of the maximum deflection vs. aspect ratios when subjected to a point load and a sinusoidal distributed load ..... 64

Figure 19: Effects of varying power indices and thickness ratios on plate’s non-dimensional fundamental frequencies of the first mode on P-FGM and S-FGM..... 66

Figure 20: Effects of varying power indices and aspect ratios on plate’s non-dimensional fundamental frequencies of the first mode on P-FGM and S-FGM ..... 66

Figure 21: Effects of varying surfaces constituents and thickness ratios on the plate’s fundamental frequencies of the first mode for a) P-FGM, b) S-FGM and c) E-FGM, from top to bottom plots, respectively. .... 69

Figure 22: Effects of varying surfaces constituents and aspect ratios on the plate's fundamental frequencies of the first mode for a) P-FGM, b) S-FGM and c) E-FGM, from top to bottom plots, respectively. .... 70

Figure 23: Effect of Shear deformation in terms of various thickness ratios on predicting the dimensionless deflections of a) P-FGM, b) S-FGM and c) E-FGM, from top to bottom plots, respectively..... 75

Figure 24: Effect of Shear deformation in terms of various aspect ratios on predicting the dimensionless deflections of a) P-FGM, b) S-FGM and c) E-FGM, from top to bottom plots, respectively..... 76

Figure 25: Effect of power index variation on the percentage increase in maximum deflection calculated using HSDT over CPT results at different aspect ratios for: (a) P-FGM and (b) S-FGM, from top to bottom, respectively..... 81

## **LIST OF ABBREVIATIONS**

FGM	Functionally Graded Materials
FG	Functionally Graded
P-FGM	Functionally Graded Materials with Power Volume Fraction Law
S-FGM	Functionally Graded Materials with Sigmoid Volume Fraction Law
E-FGM	Functionally Graded Materials with Exponential Volume Fraction Law
P-	Power Law
S-	Sigmoid Law
E-	Exponential Law
FEM	Finite Element Method
CPT	Classical Plate Theory
FSDT	First Order Shear Deformation Theory
TSDT	Third Order Shear Deformation Theory
HSDT	Higher Order Shear Deformation Theory
2D / 3D	Two or Three Dimensional, Respectively
P	Power Index for Either Power Law or Sigmoid Law
E	Modulus of Elasticity

## **ABSTRACT**

Full Name : Sultan Mohammedali A. Ghazzawi  
Thesis Title : Effect of Shear Deformation on Static and Dynamic Behavior of Thick Functionally Graded Material Panels  
Major Field : Aerospace Engineering  
Date of Degree : December 2018

Functionally graded material structures, especially panels, have various applications in the aerospace field. This research aims at studying the behaviors of classes of functionally graded material plates statically and dynamically, with emphasis on the influence of transverse shear deformations. The three most common kinds of functions describing the volume fraction, (power, sigmoid, and exponential functions), are presented. Literature review shows lack of research of the behavior of sigmoid and exponentially varying functionally graded panels. Then the kinematics of several common plate theories are presented with their associated assumptions and equations. Governing equations of both classical plate theory and third order shear deformation theory are derived and are later solved by Navier-type Fourier series expansions that resulted in closed form matrices associated to the stiffness and mass of the plate. All calculations are done on MATLAB in a manner that facilitates subsequent integration with FEM solvers. The obtained results are validated by comparisons with published results. The comparisons show excellent agreement in the case of thick functionally power FGM plates, which is extensively studied in literature. Next, a comparative study is conducted to see the effect of power indices, elastic moduli ratios, density ratios, thickness ratios, and plate aspect ratios on the maximum deflection and natural frequencies of the plate. Results show that, for power

indices greater than 1, the sigmoid-law panels always exhibit smaller maximum deflection and higher natural frequencies, compared to the exponential and power laws. Results also show similar behavior for exponential-law panels. Finally, shear deformation influence on the deflection and natural frequencies for the different types of FGM plates is illustrated. The effect of neglecting shear deformations in the classical plate formulation is quantified for different plate parameters and property variation functions. Results showed variations in the three types of property function, and greater effect for plate thickness ratio than aspect ratio. Results of sigmoid and exponential thick functionally graded plates can be used as reference for further studies because there are virtually none in the literature.



## ملخص الرسالة

الاسم الكامل: سلطان بن محمد علي بن عبد القادر غزاوي

عنوان الرسالة: تأثير تشوه القص في السلوك السكوني والحركي للألواح السميكة من المواد المتدرجة دالياً

التخصص: هندسة الطيران و الفضاء

تاريخ الدرجة العلمية: ديسمبر 2018 م

إن هياكل المواد المتدرجة دالياً، خاصة الألواح منها، لها تطبيقات مختلفة في مجال هندسة الطيران والفضاء، ويهدف هذا البحث إلى دراسة السلوك الساكن والحركي لفئات مختلفة من الألواح المصنوعة من المواد المتدرجة دالياً، مع التركيز على تأثير التشوهات القصية المستعرضة، حيث يتم عرض الأنواع الثلاثة الأكثر شيوعاً لدالات كسر الحجم، وهي دالة قانون القوة، ودالة السينية، والدالة الأسية، ويظهر المسح الأدبي نقص الأبحاث على الألواح المتدرجة دالياً طبقاً للدالة السينية والدالة الأسية، ثم يتم عرض حركيات من عدة نظريات شائعة للألواح، مع الافتراضات والمعادلات المرتبطة بها، ويتم استنتاج المعادلات الحاكمة للنظرية التقليدية للألواح، ونظرية تشوه القص من الرتبة الثالثة، وحلها لاحقاً من خلال امتدادات فوربيه لحلول من نوع نافير، والتي ينتج عنها صور مغلقة لكل من مصفوفتي جساءة وكتلة اللوح. تتم جميع الحسابات باستخدام برنامج ماتلاب بطريقة تسهل الدمج مع برامج حل طريقة العناصر المحددة لاحقاً، ثم يتم التحقق من صحة النتائج التي تم الحصول عليها عن طريق عقد المقارنات مع المتاح من النتائج المنشورة، وتظهر المقارنات اتفاقاً ممتازاً في حالة الألواح السميكة المتدرجة دالياً طبقاً لدالة القوة، والتي تم دراستها على نطاق واسع في البحوث المطبوعة. بعد ذلك يتم إجراء دراسة مقارنة لمعرفة تأثير كل من قيم مؤشر الأس، ونسبة معاملات المرونة، ونسبة الكثافة، ونسب التخانة، والنسبة الباعية للوح على الحد الأقصى لإزاحة اللوح وتردداته الطبيعية، وتشير النتائج إلى أنه، بالنسبة لقيم مؤشر القوة التي تزيد عن 1، فإن ألواح الدالة السينية تظهر دائماً إزاحة أقل، وترددًا طبيعيًا أعلى، مقارنةً بالألواح الدوال الأسية ودوال القوة، كما تظهر النتائج أيضًا سلوكًا مماثلًا في ألواح الدوال الأسية، وأخيرًا، يتم

استعراض تأثير تشوه القص على الإزاحة والترددات الطبيعية لأنواع المختلفة من ألواح المواد المتدرجة دالياً، ويتم تحديد مقدار تأثير إهمال تشوهات القص عند الصياغة التقليدية للألواح، لمختلف معاملات الألواح، ودوال تغير الخصائص. ولقد أظهرت النتائج اختلافات في حالة الأنواع الثلاثة لدوال الخصائص، وتأثيراً أكبر لنسبة الثخانة عن النسبة الباعية، ويمكن استخدام نتائج الألواح السمكية المصنوعة من مواد متغيرة دالياً طبقاً لدالة سينية أو أسية كمرجع لمزيد من الدراسات، إذ أنه لا يكاد يوجد أي منها في الأدبيات.

# CHAPTER 1

## INTRODUCTION

### 1.1 Composites and Laminated Composite

Composite materials are materials that are manufactured or combined from two or more constituents with different properties in order to have better and more reliable materials, while keeping the individual constituents designated. Historically, ancient civilizations used the concept of composites for hundreds of years. For example, bricks were made from straw and muds by the ancient Egyptian. Wattle and daub (Figure 1) is an over 6000 years old composite building material used in Europe and Australia, and it was made of wooden strips and some sort of sticky material. Furthermore, concrete is most famous composite material, because of its huge and various applications in the present time. Some of the advantages of composite materials are better strength, lower weight and cheaper operation costs. They have various useful applications such as, mortars, reinforced plastics, metal composites and ceramic composites. Those composites could be found in buildings, bridges, automotive (specially racing vehicles) and aerospace vehicles. One of the most important type of composites are the laminated composites.



**Figure 1: A house made of wattle and daub**

Laminated composites (Figure 2) combine two or more layers of different and dissimilar materials to have the required properties, such as: stiffness, coefficients of thermal expansion, and strength. One of the famous examples of those types of composites are the fiber-reinforced laminated composite materials. Since those conventional joined materials are in fact dissimilar, they tend to de-bond and form cracks, which can be found usually in weaker sections or the interface. Residual stresses can also be initiated because of the variety of thermal coefficients of each component used. To get rid of those drawbacks, a composite laminated material of continuous and gradual change of properties across the thickness were introduced by Toshio Watanabe in 1987. Since then this type of composite materials are called Functionally Graded Materials (FGM).



**Figure 2: Laminated composite specimen**

## **1.2 Functionally Graded Materials**

Functionally graded materials are essentially inhomogeneous materials, made of two or more ingredients, with engineering properties vary in a controlled manner, such that those properties will change as a function of a certain direction (usually in the thickness direction), in order to get the optimum stiffness and strength variation. Therefore, FGM materials eliminate the side effects of the traditional laminated composites which are caused by the sudden and discourteous change in the material properties (thermos-mechanical properties). In general, the two types of laminated composites are shown in Figure 3. Unlike the conventional step wise laminated composites (Figure 3b), it is clear from Figure 3a that FGM materials have continuous and gradual changes in the microstructure and composition (in volume fraction) with the thickness direction.

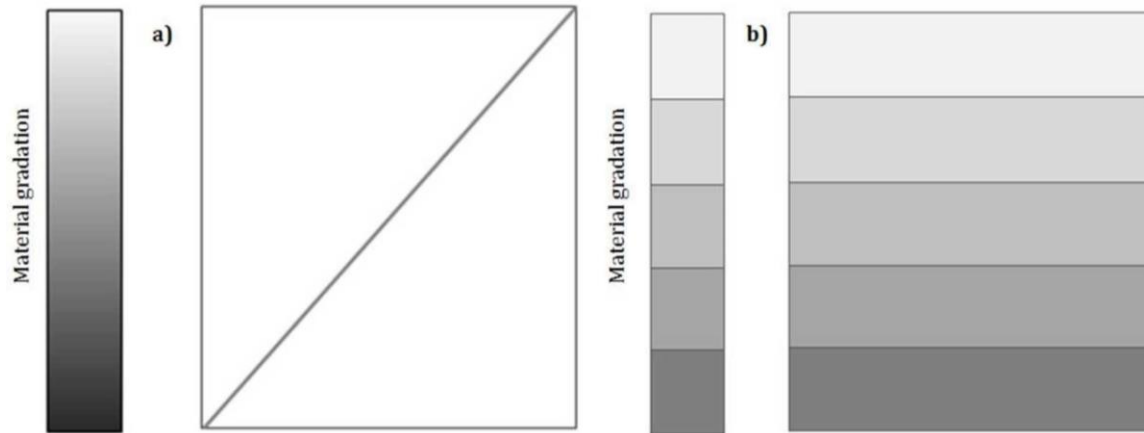


**Figure 3: Concept of composition gradation in composites [1]**

There is an increasing demand in high performance materials specially FGM materials, which have the great capability of changing mechanical and thermal properties, such as Young's modulus, for engineering use like aerospace engineering applications. For instance, the speed of a space shuttle can reach up to 25 Mach which leads to tremendous amount of heat interacting with the shuttle body (temperature can reach as high as 2000 degree Celsius), therefore; FGM materials would have a great and effective role to resist this extremely elevated temperatures due to air friction. Thermal-resisting FGM plates made of metals and ceramics are usually used on space shuttles, since the ceramic part provide high level of heat resistance because of low heat conductivity, while the parts made of metals will provide fracture resistance caused by fast and rapid temperature changes due to the ductility feature of that metal. Another main application is the materials made in the manufacturing of the combustion chamber of an engine, since temperature can exceed 2000 degree Celsius. Furthermore, FGM are used in nuclear powerplants

Bond strength can be developed by using FGM in the interface layer between two dissimilar material. Moreover, thermal and residual stresses, specially stresses at interface

and endpoints, could be reduced or even eliminated by coating and interfacing using FGM, which also leads to the reduction of crack initiation possibilities.

FGM can be classified depending on its components combinations, their changing compositions, the density gradient, and the application fields. First for components combinations, FGM can be made of metal-ceramic, ceramic-ceramic, etc. Second, it can be classified according to changing compositions as gradient type, coating type and connection type. Then, for the density gradient classification, FGM is divided into optical FGM, fine FGM etc. Finally, it can be categorized according to its applications, such as biological FGM, chemical FGM, electronical FGM or heat-resisting FGM. Refer to Table 1 for more information regarding the famous type of FGM and their applications.

**Table 1: Widely used types of FGM and their applications [1]**

Sl.No	FGCM type	Requirements	Application
1	SiC-SiC	Corrosion resistance and hardness	Combustion chambers
2	Al-SiC	Hardness and toughness	Combustion chambers
3	SiCw/Al-alloy	Thermal resistance and chemical resistance	CNG storage cylinders, Diesel Engine pistons
4	(E-glass/epoxy	Hardness and damping properties	Brake rotors, Leaf springs
4	Al-C		Drive shafts, Hubble space telescope metering truss assembly, Turbine rotor, Turbine wheels
5	Al-SiC		Flywheels, Racing car brakes
6	SiCp/Al-alloy	High melting point, low plasticity and high hardness	Motorcycle drive sprocket, Pulleys, Torque converter reactor, Shock absorber
7	Carbon and glass fibers		Propulsion shaft
8	Glass/Epoxy		Cylindrical pressure hull, Sonar domes
9	TiAl-SiC fibers		Composite piping system, Scuba diving cylinders
10	Be-Al		Floats, Boat hulls. Wind tunnel blades, Spacecraft truss structure, Reflectors, Solar panels, Camera housing
11	Al <sub>2</sub> O <sub>3</sub> /Al-alloy	Good thermal and corrosive resistance	Rocket nozzle, Wings, Rotary launchers, Engine casing
12	Carbon/Bismaleimide		Drive shaft, Propeller blades, Landing gear doors, Thrust reverser(Heat exchanger panels, Engine parts
13	Carbon/Epoxy	Lightweight and good damping properties	Helicopter components viz. Rotor drive shaft, Mast mount, Main rotor blades
14	SiCw/6061	Hard and toughness	Racing bicycle frame, Racing vehicle frame.
15	(Al-alloy/CNT),	Light weight and high stiffness	Artificial ligaments, MRI scanner cryogenic tubes, Wheelchairs, Hip joint implants, Eyeglass frames, camera tripods, Musical instruments

### 1.3 Classification of FGM Plates

Plates that are made of functionally graded materials can be classified based on various aspects, such as processing or the way of who materials are changing across the thickness. The last way, which called classification by material gradient, is the most common way for FGM identifying FGM Plates. These plates are manufactured such that the building blocks, or the components vary across a one dimension, usually is the thickness, in an identified manner. along with this variation in material across the thickness, material properties in macro scale also changed in a predetermined way. There are three most common ways



(volume fraction functions) of how those properties change, which are power, sigmoid and exponential functions.

The functionally graded material panel that manufactured according to a volume complies with a power function is classified as P-FGM. The properties such as mass density and modulus of elasticity alter across the thickness by the rule of mixture in a power-function manner. Figure 4 demonstrates how such properties, specifically for Young's modulus, change with the thickness direction for an FGM plate that has a z-axis directed toward the bottom. As it is shown, the change in the elasticity is almost sudden closer to the lower surface for a power index (P) greater than one, to be more specific, the greater the power is the sudden the change is, also the closer the change is to the bottom layer. In addition, vice versa is true for power indices between zeros and one. Most of published research work is conducted on P-FGM plates.

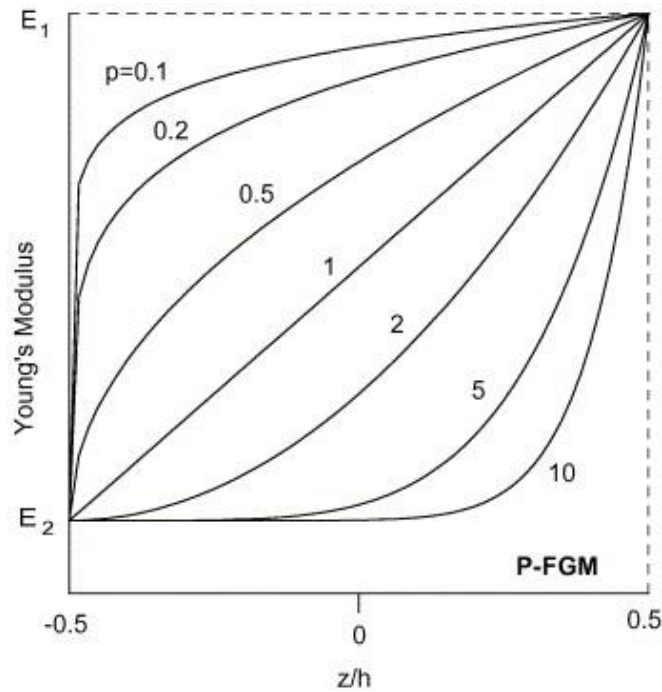


Figure 4: Effect of Power Law on Young's modulus Across the Plate Thickness [2]

Another type of FGM panel is called sigmoid FGM plates or simply S-FGM. The creation of this kind of classification was motivated by Chung and Chi [2] from the fact that merging P-FGM, where the volume fraction is expressed as a single function, in more complex structures such as multi-layered structures, can ignite cracks. This could happen due to areas high intensity of stresses, such as interface areas where a sudden change in material properties occurs. The volume fraction of this class of FGM is expressed as a double power function, where the plate is divided basically to two parts: upper and lower parts, and each part has its own power law volume fraction function. Therefore, with this configuration as shown in Figure 5, a gradual variation in properties is secured for those complex structures.

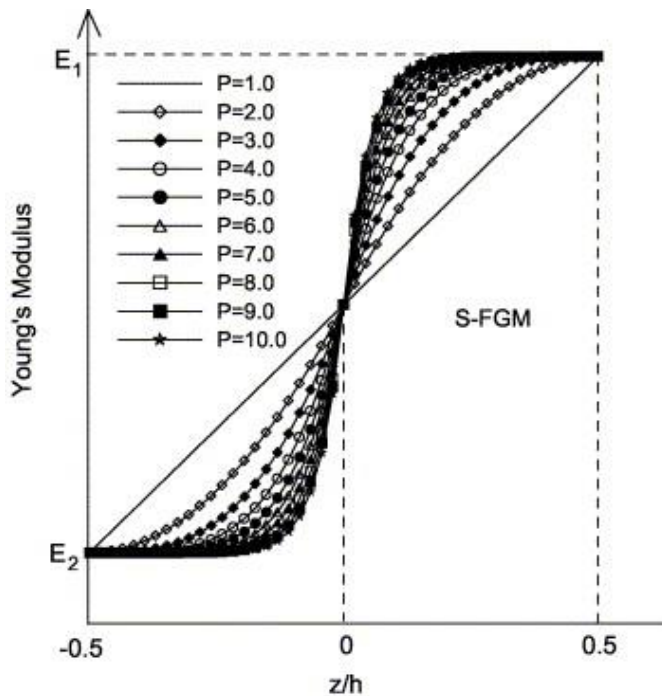
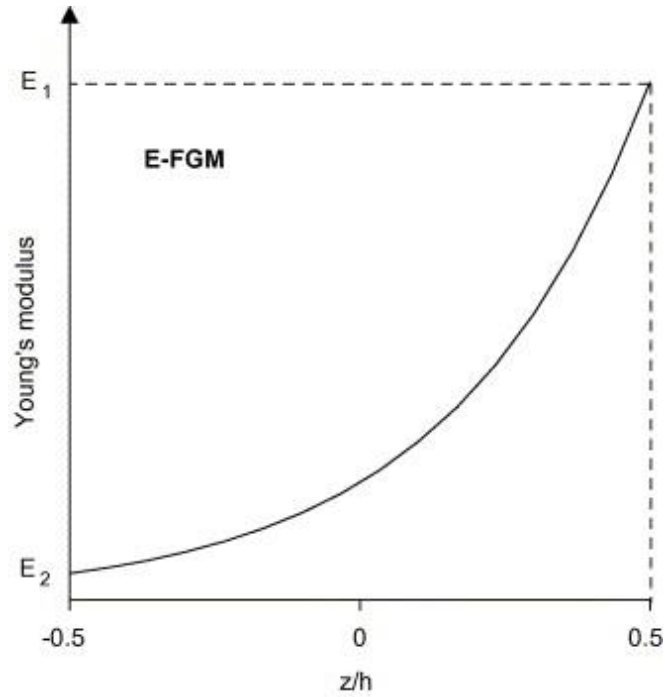


Figure 5: Effect of Sigmoid Law on Young's Modulus Across the Plate Thickness [2]

The last type of volume fraction functions is the exponential function. This kind of volume fraction is mainly used with studying the fracture behavior. It simply represents

who a material macro-property varies across a direction is an exponential style as shown in Figure 6.



**Figure 6: Effect of Exponential Law on Young's Modulus Across the Plate Thickness [2]**

This thesis deals with all the three-mentioned volume fraction variation functions. However, because of the nature of published research work, the model validation will be done only for P-FGM plates.

## **CHAPTER 2**

### **LITERATURE REVIEW**

#### **2.1 Research on Static and Dynamic Response of FGM Structures**

Functionally graded materials idea was introduced firstly during the middle of 1980s for having heat resistance barrier materials. Since then, FGM researches were developing rapidly with the help of computer programs software and the increasing industrial demands. K. Swaminathan et al. [3] made a comprehensive review paper on stress, vibration and buckling analysis of FGM plates, which summarizes the development and recent research on statics and dynamics of FGM plates. Good amount of research is done to study the mechanical and thermal behavior of FGM. It was found that adding an appropriate FGM layer to the plate would decrease the effect of compressive and tensile stresses on both surfaces of a of a simply supported homogenous plate under a surface load. However, three dimensional solutions become increasingly difficult to solve for other boundary conditions, especially when the power law is utilized to represent the distribution of constituent's volume fraction. Therefore, two dimensional simplifications were implemented in these cases.

Smart functionally graded plates were analyzed through three dimensional techniques by Reddy and Cheng [4]. The smart plate consisted of a metal-rich part connected to actuators made of an active material and a ceramic-rich part. While Thermo-mechanical loads are subjected to this plate, stresses, displacements and vibration amplitudes are

controlled by the actuators. Throughout this paper, three dimensional asymptotic solutions are obtained for bending the smart plate by utilizing the transfer matrix and asymptotic expansion techniques. Numerical results are given by the help of Mori-Tanaka scheme for estimating the local effective material properties. From the given numerical results of three-dimensional distributions of displacements and stresses for various volume fraction of the smart FGM plate, it was found that the effect of volume fraction distributions is only important for the temperature field.

Vel and Batra [5] proposed a 3-D exact solution to model both forced and free vibration of a plate that was rectangle and made of FG ingredients with an assumption that the volume constituent fraction and the material effective property varies in its thickness direction. The equation governing the steady-state vibration was reduced by applying a suitable displacement function that satisfies its boundary condition into a group of coupled differential equations which was solved through the power series method. The material effective property at a point was obtained through volume fractions while the material property that constitutes its phases was obtained through the self-consistent scheme, Mori-Tanaka method or by combining both methods. Results for functionally graded thick plate showed sententious differences amidst the proposed exact solution and the classical plate theory but correlated with the third and the first order from of shear deformable theory. The exact solution present was a benchmark to evaluate the adequacy of various theories of plates and their approximate solutions.

Zenkour, [6] employed the generalized theory of deformation associated to shear effects derived by other author to evaluate the responses of an FGM rectangular simply supported plates under transverse static loading condition, by simply enforcing conditions

of traction-free boundaries at the plate faces without any use of transverse correction factors such that an accurate transverse shear strain was presented with an assumption that the material properties vary throughout the material thickness-wise direction which correlates with simple power function expression in terms of volume gradient of its constituent elements. The equilibrium equations were given by the generalized shear deformation theory, and the numerical illustration that relates its bending response to two components. Contributions from plate aspect ratio, transversal deformation volume fraction and side-to-thickness ratio were also investigated. In his work, he presented a generalized formula using the shear deformation theory with identical dependent variables contained in first order theory with a better prediction of functionally graded material stress analysis, deflection and satisfy the boundary condition of zero tangential traction. The presented theory and the theory of higher order avoided the use of shear correction factor while the governed partial differential equations were simplified to the ordinary differential equation and solve using Navier solutions approach for the simply supported plate. The responses of deflection and stress of functionally gradient plate were studied while applying uniform loading condition with an assumption that the properties of the ingredients are gradually varying across the thickness, and it was found the basic response that corresponds to the properties intermediate of the material constituents lie in-between and the result doesn't vary with changes in boundary conditions.

Ordinary analytical methods for investigating transient thermal loads on FGM plates is quite difficult, therefore, Laplace transforms, and perturbation methods were used to study those types of loads on FGM plates analytically. Many researches focused on thermo-elastic plastic behaviors of FGM plates for linear and non-linear compositional relations,

see for example [7]. They found that, reducing or even getting rid of the unwanted stress on several crucial locations could be achieved by controlling the variation of volume fraction across the thickness of FGM plates. For FGM shell structures under thermal loads, the temperature profile is non-linear even for thin shells. In case of FGM thick plates, a thermo-elastic study was conducted using differential quadrature and state space methods.

Simisk [8] study was interested in how FGM beams would respond freely (free vibration) under different boundary conditions. The research based on power law distribution of the volume fraction and the material properties. Moreover, several theories of displacement field, such as first and third orders shear deformable theories were implemented in order to come up with two different sorts of formulation. The study utilized Lagrange's equations and multipliers for solving the equations associated with finding unforced frequencies of the FGM beam. The investigator came up with several results, such as in case of thicker beams, frequencies calculated by CPT would significantly differ from TSDT. Furthermore, beam's frequencies are inversely proportional with the power indices and the slenderness of the indicated beam, but not for longer beams.

Researches have also covered several other shapes, such as shells made of doubly-curved FGM. One of remarkable work was done by Tornabene, et al. [9], which was, the first of its kind in the literature, aimed to cover the dynamic characteristics. They depended on various theories with higher orders along with the method of Generalized Differential Quadrature (CDQ) for solving the equations of motions. The study succeeded to solve for fundamental frequencies and mode shapes of various types of structures with comparative study between their result and the published ones.

## 2.2 Research of FGM Plates Responses Using CPT

Classical plate theory is considered as the simplest form of describing plate's displacement field. Therefore, Implementations of classical plate theories have been widely spreaded for determining either static or dynamic responses of plates, though it might ended up with significant error if it is applied to thick plates.

Javaheri and Eslami [10] formulated stability and equilibrium equations of rectangular FGM panels that had simple supports, and manufactured from metal and ceramic elements utilizing the classical theory of panel structures (CPT). It was found that those relations actually are very similar to the equations of homogeneous isentropic plates. Then, thermal buckling analysis of these FGM plates was conducted for four different thermal load situations, which led to closed form solutions. Those four cases were, thermal buckling of gradient composite plates undergoing a uniformly temperature jump, linear variation of temperatures across the thickness, non-linear changes of temperatures throughout the thickness, and linear variation associated to cross-length temperatures. It was concluded from this paper that the critical temperature change of buckling  $\Delta T_{cr}$  of FGM plates is, in general, lower than homogeneous plates. Moreover,  $\Delta T_{cr}$  is inversely proportional to the index of power law and the dimensional aspect ratio  $b/h$ , while it is directly proportional to the dimensional ratio  $b/a$ . By breaking down and analyzing heat conduction equation, the allocation of thickness-wise temperature of the plate was found to be nonlinear. In addition,  $\Delta T_{cr}$  for linear temperature changes through the length is doubled compared to the constantly change of temperature. Unlike  $\Delta T_{cr}$  for homogenous plate,  $\Delta T_{cr}$  of FGM



plates for temperature changes across the length was found to be higher than the temperature differences of linear form through the plate's height.

A closed form relation, supported with numerical solutions for rectangular simply supported FGM plate obeying the power law (P-FGM), exponential law (E-FGM) and Sigmoid law (S-FGM) were derived by Chi and Chung [2] and [11]. The effect of a transverse load on a simply supported elastic medium-thick rectangular functionally graded material plate, where the classical plate theory was used along with Fourier series expansions, were discussed. Results were benchmarked with those from finite element methods for validation purposes. Several conclusions were made from that investigation. For instance, it was found that the derived formulas are also applicable to isotropic plates. Moreover, they were able to prove that there is a strong relation between the location of the neutral plane and the ratios of modulus of elasticity, but, this relation is negligible between the neutral plane location and the other parameters, such as applied loads and plate dimensions.

Ashrafi H.R et al. [12] employed the method of finite elements to evaluate the frequencies linked to resonance and mode shape through modal analysis on the functionally graded material. A Matlab code was written and embedded through ABACUS on the FEM while the simulated code for other researcher work was model to validated results obtained in the presented method. The newly proposed finite element method to the modal analysis of rectangular functionally graded material plates is based on classical and Kirchhoff plate theory with assumption that the material properties vary throughout the thickness side in accordance with simple power function of distributions such that the influence of the power index on functionally graded natural frequency and mode shape were investigated for

different boundary conditions. It was inferred from the obtained results that mode shapes and natural frequencies were of high accuracy for user-written subroutine as well as for the finite element method results presented in his work. After that, the effects of material type and clamping condition (i.e the parameter 'n') were examined such that increase in natural frequency is associated with a decrease in the parameter 'n' whereby ceramics phase in functionally graded plate increases while the metal phase decreases leading to an increase in plate stiffness.

### **2.3 Research of FGM Plate Response using FSDT**

A more developed form of CPT is called the theory of first order theory of shear deformation FSDT. This theory accounts for the shear effects across the thickness direction of a plate. Therefore, it is obvious that it is used with thicker FGM plates for obtaining much more accurate outcomes.

Free vibration behavior of FGM plates was further put under consideration with Zhao, et al [13]. They used a method called element-free kp-Ritz method, which was utilized previously with composite and isotropic analysis. The study investigated on skew and rectangular plates made of four different combinations of metal-ceramic FG materials, with volume fraction and material features vary powerly in thickness-wise direction. The First order theory of shear distortion was used along with Ritz method in order to obtain the desired equations of stability. Outcomes tied to how various cases of boundary conditions, power indices and length to thickness ratios could affect the free response of the plate. While confirmed with the obtained results from literature, the outcome of the study concluded several aspects. First, for rectangular plates, natural frequencies tended to be

independent from the power indices when varying the plate length. However, the variation power index has a significant influence on the free vibration response when it is less than 5. Finally, angles of skew affect skew panels, which has angles more than 30 degrees, severely on the natural frequencies. Moreover, there was no evidence during their study that showed strong effects on plates free response, when shear factor of correction is varied.

Dynamic free responses of an FGM plate that have a power law volume distribution across the thickness was observed by Hosseini-Hashemi et al. [14]. The plate was assumed to supported in a simple manner in two edges which oppose each other, while the other two edges encountered several types of supports. Shear deformation theory in its first order form was implemented in the procedure of deriving the equilibrium equations. However, authors derived a different correction factor based on Mindlin theory of plates. Accurate results were confirmed through comparative studies, and they showed how the correction factor is related with the thickness of the plate. They end up with claiming that the obtained outcomes could be used for later comparative study, since the precision of the results, which discussed also the influence of aspect ratios, power values, and thickness variation on the free vibration behavior, were guaranteed.

Thai and Choi [15], along with Belifa, et al. [16] tried to simplify the traditional first order theory of shear deformation (FSDT) in order to observe the associated results for the behavior of FGM panels associated with static and dynamic situations. Their studies were conducted under several assumptions, which are: the Cartesian coordinate systems emerged from the plate's neutral plane, strains were negligible due to relatively small displacements compare to the thickness and crosswise normal stresses can be ignored. The plate is also assumed to be supported in a simple manner, with power law function

controlling its volume fraction throughout the thickness. To obtain equations that govern the plate behavior, displacement field of FSDT is simplified by getting rid of the effect of stretching-bending coupling, so that the unknowns become one less than the original theory. Moreover, implementation of the principle of Hamilton along with Navier's solutions on the simplified version of FSDT allowed the formulation of the equations of motion. With verified results, the authors of both papers were able to come up with different results and conclusions. It was claimed that, the obtained simplified version of the first order theory displacement field is adequate for investigating how panels behave in term of free vibration and deflection behaviors, without losing accuracy because of simplicity.

## **2.4 Research of FGM Plate Response using HSDT**

Various researches and studies were made for mechanical behavior of plates utilizing either 2-D or 3-D higher order theories. All versions of those theories would provide high amount of accuracy and precisions for thicker plates.

TSDT, which refers to the third order formula of shear deformable plates, was used by Reddy [17], in order to form an analytical solution by Navier's method for plates (rectangular shaped) and a finite element model. Moreover, the harmony and the accuracy of outcomes of by classical plate theory (CPT) and the two-dimensional elasticity theory were proved by some researches using finite element method. Coupling by thermo-mechanical techniques, time dependency and von Karman-type geometric nonlinearity was considered in solving the equations. Then, effects of the variation of constituents' concentrations and elastic moduli ratios of the ingredients on deflections and shear stresses in the transverse direction were presented based on Navier's solutions for plates that are

simply supported. It was found that when only mechanical loads are deployed on a plate, the dynamic response of the mid-surface lies in between of the FGM plate components. However, this is not true when both thermal and mechanical loads are applied. Overall, the response of intermediate planes of the metal-ceramic FGM plate does not necessarily fall in between (intermediate) the responses of the metal and the ceramic parts.

Qian et al. [18] employed theories of transverse shear distortion with higher order forms and a meshless confined Petrov-Galerkin method to analyze the dynamics and static deformation of a thick functionally graded elastic plate manufactured from isotropic constituents with an assumption that the macroscopically isotropic material properties vary in the thickness direction. The relative change in the material nature of the functionally graded material is associated to the changing of the volume gradient of the material respective constituents that achieved by manufacturing techniques e.g. high-speed centrifugal casting, direct oxidation techniques to mention but few. Defects were observed from earlier work that employed first or third order coupled with finite element method with the assumption that neglect the transverse normal deformation and that deformation plane stress state is best in the plate. Only thin plates are suited with these assumptions. Boundary conditions were set for simply supported, free and clamped while St. Venant principle was invoked which state that computed solutions are valid at any point away from the edges. The code was developed to analyze statically the deformation of forced and free vibration of thick functionally gradient composite plates while being substantiated by correlating results for homogenous plates with the analytical technique of the analogous problem. For both static and dynamic loads, measured resonance frequencies of the functionally graded panels were found to reasonably align with values found analytically,

such that no significant effects of the material property gradient on the fundamental natural frequency.

Investigations on natural frequencies and stresses associated with buckling of FGM plates were conducted by Matsunaga [19]. Several effects were involved in that study, such as transverse shear (variable thickness ratios), normal deformation and rotational inertia, where the functionally graded plate itself obeyed the power law (P-FGM) of volume distribution (through thickness direction), and the plate was assumed to be simply supported. The governing equations for plates undergoing in-plane stresses, deduced from two-dimensional higher order relations, were obtained using Hamilton's principle. Those equations were then solved based on series expansion, in order to solve the eigen value problem. Validation with older published works was done for natural frequencies and stresses. This study was able to confirm various fruitful outcomes. First, accuracy of the obtained results was confirmed. Moreover, through the mentioned study, theories of higher orders were proved to be quite precise. Other products were obtained in thickness-wise direction, such as components of stresses, modal displacements distribution, and modal stresses in transverse directions. It was concluded that the prediction of several essential aspects related to FGM plates can be highly accurate, when the provided two-dimensional higher order theory is implemented to gain natural frequencies, stresses belong to buckling, displacements distribution and components of stress.

Several researches were conducted in favor of FGM sandwich plates. For instance, Natarajan and Manickam [20], investigated how accurate are the results obtained by higher order theories for different types of sandwich plates, such as FG cores with isotropic faces or vice versa, taking into their account the variation on power indices or thickness ratios.

They concluded that HSDT theories are more accurate, but lower theories are still a good choice for simplicity. Moreover, a innovative new higher order theory was introduced by Bessaim et al. [21]. The new theory used for studying the mechanical behavior of symmetric and non-symmetric plates made of FGM faces. With simply supported condition in all boundaries, the new theory, which has less number of unknowns (simplicity), proved to be accurate. Furthermore, the proposed method succeeded to exclude factors account for correcting the shear effects. They concluded that, the study would open new opportunities of observing sandwich FGM plates behaviors in much more simple manner. Similarly, that simple higher order theory that contain less unknowns and therefore, less equations, were later used, but for observing FGM rectangular plates bending behavior and free responses instead of FGM sandwiches, by Belabed et al. [22]. They ended up with similar conclusions as for sandwich FGMs, which is the great feature of simplicity and accuracy that the new method has, even for high thicknesses.

Akbarzadeh et al. [23] performed analytical and comparative study between FSD and TSD theories of rectangular plate. The response, in static and dynamic manner, of the plate was deduced using power law FGM plate in the thickness wise. The equations of motion were built according to Fourier expansion and Laplace transformation techniques. The results then constructed after inversion from Laplace domain to time domain, along with numerical integrations that depend on Newark method. Statics, and Forced and free dynamics responses were mentioned and verified. It was ended that rising up the power index leads to higher deflection. Moreover, the longer the plate is, the less significant is the difference between first or higher order theories.

Hosseini-Hashemi, et al., [24] proposed an exact procedural closed-form based on Reddy's theory of the third order form to analyze the free vibrations of thick FG plates , which is simply supported on its either edges, with an assumption that the mass density and modulus of elasticity varies by the power function, whereby it's Poisson ratio is constant. Ng et al. were first to consider the stability of FGM dynamically without consideration about thermal environmental influence and the aerodynamic loading effects which cause inadequacies to substantiate the validity of result from CPT because it's overestimated frequencies and underestimated deflection. Shear deformation factor used for the theory of plates for Mindlin was gained for functionally graded plate where the Hamiltonian principle was employed to extract the dynamic equilibrium equations and setting its natural boundary conditions. Introducing the potential functions and variables separation method, the solution of exact with close form for the in-plane and out-of-plane defections was determined. It was observed that the that result obtained from the newly proposed exact closed-form commute well while in comparison with existing literature and result obtained through 3-D finite element model and that the newly proposed method accurately predict both the in and out planes features of the functionally composite thick plate influences from plate parameter such as aspect and thickness ratios, power indices and conditions of the boundary on the natural frequency parameter were clearly investigated.

Mantari et al [25], [26] and [27] studied intensively the effects of implementing new evolved versions of higher order theories on FGM plates' static behavior. They provided a detailed comparison between traditional and new theories. Moreover, their observations were mainly based on two types of volume fractions, which are exponential and power



laws, along with simply supported panels. To derive the equations of motions, the idea of virtual work was implemented, along with Navier solutions. The overall precision of the proposed new theories, called trigonometric shear theories with higher orders, was proved effectively specially for thick panels.

Ismail et al. [28] applied Four-variable refined theory to evaluate the analytical solution of dynamic and static deflection of the functionally graded plate while employing a new function  $\psi(z)$  for analyzing deflection statically and dynamically for the plates. In recent times, researchers give more attention to analyze the nature of functionally graded materials applying various loading conditions while testing numerous plate theories. The classical plate theory employed in its analysis with assumption that the traverse shear effect is negligible has underestimated the deflection and overrated frequencies and buckling load for moderately thick plate but provides a reasonable result for thin plates such that shear deformation, bending shear coupling and extensional bending are essentials to the instability and failure of composite structures, obtaining more practically reasonable results and predictions of the functionally graded plate the new Four-variables refined plate theory among others were derived to compensate for the deficiencies faulted on the classical theory of panel structures. The Four-variable refined theory was developed to use the mentioned new function, in order to observe the mechanics of FG plates and the result obtained was validated with present literature the employed the first or other higher orders forms, along with the traditional theory, CPT. The newly developed theory which employed the use of a new function  $\psi(z)$  in analyzing mechanical responses of such composites was moa del. The validated obtained results was found to commute well with Reddy's solution.

SiddaRedddy et al [29], looked for the shear deformation influence on FGM panels by utilizing a higher order displacement field that omits the shear correction factor. The plate was assumed to follow power gradient pattern, and, it was supported simply. Virtual work and Navier techniques were applied for gaining the desired governing equation. The utilized method agreed accurately with pervious works, which indicated the high accuracy of their results. It was concluded that plates behavior affected significantly with changing the concentration of the constitutes.

Effects of buckling and unforced dynamic response on FGM rectangular plates with several thicknesses were also examined by Thin, et al. [30]. The examined plate was assumed to be supported simply and followed the general power law of volume fraction. For obtaining the governing equations, several steps were taken by the investigators. First, they used a higher order theory for displacement field of the plate that has 12 unknowns in it. However, the number of unknowns was able to be reduced by 4 ending up with 8 unknowns only, since crosswise shear stresses at the top and the bottom on the plate were assumed to be negligible. Then, from constitutive relations and principle of Hamilton, governing equations were derived successfully. Finally, by adopting Navier's methods for simply supported plate structure, the governing equations were solved, and several interesting outcomes were obtained. After verifying the results with those which were obtained previously in older papers, the following outcomes were guaranteed. First of all, results obtained were accurate because they matched precisely with the literature. Second, variation of the power index and length-to-height ratio confirmed the effectiveness of them on the buckling and dynamic natures of FGM plates. Finally, the research concluded that power indices have significant effects on buckling loads and natural frequencies since

increasing the index also leads to an increase in buckling loads, while that would affect totally in an inverse way for the natural frequency.

## **2.5 Motivation and Objective**

It can be seen that, FGMs have great potential to play a major role in future of engineering applications. After going through recent research regarding plates' behavior made of functionally graded ingredients, the following research gaps are found:

1. Most of those studies were using simple 2D theories like first or third orders theories of shear deformable theories, because they could give quite accurate results with less computational efforts. Therefore, more studies and research are required to fulfill the current gaps in this area. For instance, the use of higher order theories for investigating the impact of nonlinearity of geometries on FGM plates could help in improving FGM researches.
2. The study of FGM plates with complex loads and boundary conditions is also quite missing.
3. Advanced computational methods using numerical techniques for three dimensional FGMs are required too.
4. Stability analytical solutions using 3D elasticity theories could have a great contribution on FGM developments.
5. Sigmoid and Exponential laws types of FGM plates (S-FGM and E-FGM) are either missing, for the cases of S-FGM, or in shortage, such as in E-FGM, of analytical solutions for various mechanical properties and behaviors.

Hence, the main objective of this work is to investigate the influence of including the shear deformation effect on the accuracy of calculating maximum deflections and natural frequencies of the three main types of FGM; namely S-, P-, and E- FGM and compare how these classes would be influenced by the shear effect. Therefore, the generated results and outcomes can be used as a benchmarking, precisely for the behaviors of those missing volume fraction functions, which are sigmoid and exponential functions. To achieve this objective, the following tasks are preformed:

- Study the difference between Third order theory of shear deformation and the classical small-deflections plate theory, that can be used to model the response of FGM Plates.
- Construct the governing equations, based on these models, of FGM plates under static or dynamic cases.
- Use appropriate methods for solving those governing equations for the maximum displacements, and natural frequencies for these classes of plates.
- Study effects of encountering the shear deformations on the results by comparing calculated values to available experimental or simulation results.

## **2.6 Thesis Organization**

The following chapters of this thesis try to achieve the above-mentioned objectives. First, chapter 3 discusses the differences between the most common plate theories and what assumptions are those theories built from. Later at the same chapter, the focus would shift to build and solve the governing equations of CPT and TSDT, in order to observe the transverse shear deformation effects on the statics and dynamics of classes of FGM.

Chapter 4 verifies the accuracy of the obtained TSDT results by comparing them with existing results from the literature. Then, comprehensive parametric studies that show the effects of changing certain factors on the general behaviors of P-, S- and E-FGM panels are conducted. Chapter 5 takes care of a comparative study between CPT (no shear effect) and TSDT (with shear effects) outputs to show the degrees of potential errors that might happen when CPT is utilized for FG plates' mechanical behaviors predictions. Finally, chapter 6 summarizes and concludes this work, then provides potential future studies.

## CHAPTER 3

### MATHEMATICAL FORMULATION OF FGM PANELS

#### 3.1 Kinematics of Different Plate Theories

Composites made of materials that are gradually and functionally vary across the thickness are commonly used as two-dimensional structures like plates. Therefore, an adequate brief review of theories for analyzing plates is necessary. These theories are divided into two major categories. The first is the two-dimensional elasticity theories, including classical theory of panels (CPT) with first order (FSDT) and third order (TSDT) shear deformation theories. The second category comprises the three-dimensional elasticity theory.

Consider a rectangular solid plate having  $a$ ,  $b$  and  $h$  as length, width and thickness respectively, where length and width is much larger compared to the thickness, as shown on Figure 5, using Cartesian coordinates, the origin is positioned in the plate center. The displacement components on  $x$ ,  $y$  and  $z$  axes of this plate is described as  $u(x, t)$ ,  $v(y, t)$  and  $w(z, t)$ , where  $t$  denotes to time. Let the strain-displacement relation be:

$$\boldsymbol{\varepsilon}(X, t) = \mathbf{D}\mathbf{u}(X, t) \quad (3.1)$$

Where  $\boldsymbol{\varepsilon}$  represents vector of strains,  $\mathbf{D}$  is the compatibility matrix and  $\mathbf{u}$  is the vector of displacements.

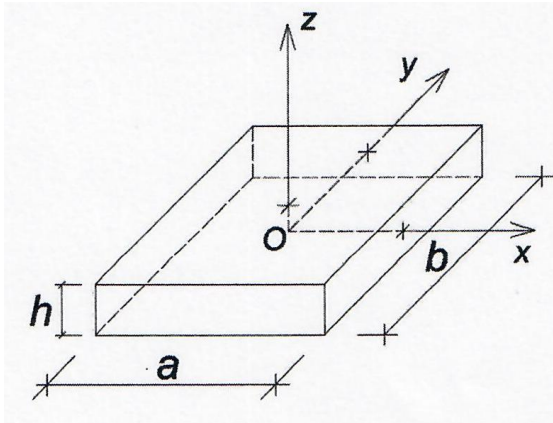


Figure 7: The coordinate system of a rectangular plate [31]

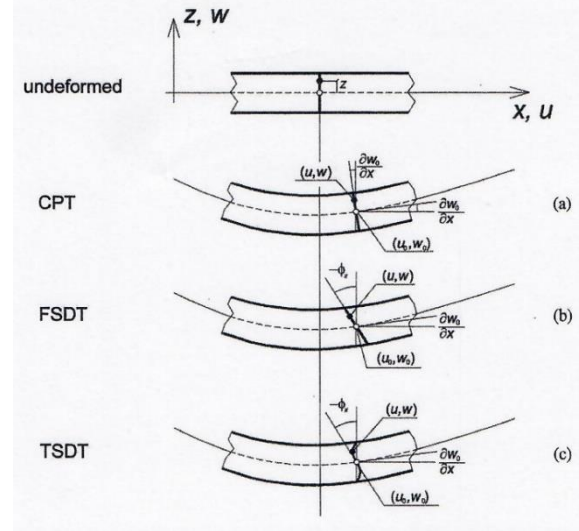


Figure 8: Concept of the deformation of a transverse normal for the elastic plate theories [31]

Generally, 2D elastic theories are simplified forms of the 3D theory with the main assumption of thin plate. Thick plates are defined as plates having the thickness to the smaller span length (length) ratio approximately more than 1/20 ( $h/a > 0.05$ ), while the thin plate is the opposite. The simplest theory of 2D theories is the classical plate theory or CPT, which is also known as the small-deflection theory of bending thin plates. Main assumptions of CPT are:

- Small mid-surface displacements compared to the plate thickness are considered, so the deflected surface slope is small and can be neglected.
- After bending, the mid-surface of the plate is unaffected with strain, means it will remain the neutral plane.
- After bending, plane sections which were initially normal to the midplane remain normal, which implies the shear (transverse shear) and normal strains are negligible.

➤ Neglect the transverse normal stress due to its small value.

These assumptions lead to the following displacement field for CPT:

$$u(x, y, z, t) = u_0(x, y, t) - z \frac{dw}{dx} \quad (3.2)$$

$$v(x, y, z, t) = v_0(x, y, t) - z \frac{dw}{dy} \quad (3.3)$$

$$w(x, y, z, t) = w_0(x, y, t) \quad (3.4)$$

Where  $u_0$ ,  $v_0$  and  $w_0$  displacements of mid-surface on x, y and z axes. (see Figure 8a), and the components of the strain displacement relation shown in equation (3.1) are as follow:

$$\mathbf{u}(X, t) = [u_0 \quad v_0 \quad w_0]^T \quad (3.5)$$

$$\boldsymbol{\varepsilon}(X, t) = [\varepsilon_{x0} \quad \varepsilon_{y0} \quad \gamma_{xy0} \quad X_x \quad X_y \quad X_{xy}]^T \quad (3.6)$$

$$\mathbf{D} = \begin{bmatrix} \partial/\partial x & 0 & 0 & 0 \\ 0 & \partial/\partial y & 0 & 0 \\ \partial/\partial y & \partial/\partial x & 0 & 0 \\ 0 & 0 & -\partial^2/\partial x^2 & 0 \\ 0 & 0 & -\partial^2/\partial y^2 & 0 \\ 0 & 0 & -2\partial^2/\partial x\partial y & 0 \end{bmatrix} \quad (3.7)$$

Where  $\varepsilon_{x0}$ ,  $\varepsilon_{y0}$  and  $\gamma_{xy0}$  are strains caused by in-plane displacements.  $X_x$ ,  $X_y$  and  $X_{xy}$  denoted to curvatures caused by the first order terms.

Some of the first third orders shear theories of plates' deformation can be considered as 2D elasticity theories for plates. Both are actually modified versions of CPT, in order to encounter the effect of transverse shear and normal strains with all other assumptions of CPT being applied. The main difference between first order (FSDT) and third order (TSDT) shear deformation theories is that FSDT require a correction factor of shear effect, since the transverse shear strains are included in the relations as constant. While TSDT



does not need that shear factor, since the transverse shear are already there in the equations as a quadratic term.

The formulas for the first order theory are:

$$u(x, y, z, t) = u_0(x, y, t) + z\phi_x(x, y, t) \quad (3.8)$$

$$v(x, y, z, t) = v_0(x, y, t) + z\phi_y(x, y, t) \quad (3.9)$$

$$w(x, y, z, t) = w_0(x, y, t) \quad (3.10)$$

Where  $u_0, v_0$  and  $w_0$  are the mid-surface displacements of a point on that surface (see Figure 8b). The rotation functions are defined as  $\frac{\partial u}{\partial z} = \phi_x$  and  $\frac{\partial v}{\partial z} = \phi_y$ .  $u_0, v_0, w_0, \phi_x$ , and  $\phi_y$  are called generalized displacements. However, for thin plates  $\phi_x$ , and  $\phi_y$  should be  $\phi_x = -\frac{\partial w_0}{\partial x}$  and  $\phi_y = -\frac{\partial w_0}{\partial y}$ . The elements of strain displacement relations are as follow:

$$\mathbf{u}(X, t) = [u_0 \quad v_0 \quad w_0 \quad \phi_x \quad \phi_y]^T \quad (3.11)$$

$$\boldsymbol{\varepsilon}(X, t) = [\varepsilon_{x0} \quad \varepsilon_{y0} \quad \gamma_{xy0} \quad X_x \quad X_y \quad \gamma_{xz0} \quad \gamma_{yz0}]^T \quad (3.12)$$

$$\mathbf{D} = \begin{bmatrix} \partial/\partial x & 0 & 0 & 0 & 0 \\ 0 & \partial/\partial y & 0 & 0 & 0 \\ \partial/\partial y & \partial/\partial x & 0 & 0 & 0 \\ 0 & 0 & 0 & \partial/\partial x & 0 \\ 0 & 0 & 0 & 0 & \partial/\partial y \\ 0 & 0 & 0 & \partial/\partial y & \partial/\partial x \\ 0 & 0 & \partial/\partial x & 1 & 0 \\ 0 & 0 & \partial/\partial y & 0 & 1 \end{bmatrix} \quad (3.13)$$

Where  $\gamma_{yz0}$  and  $\gamma_{xz0}$  are shear strains caused by first order terms.

Third order deformation theory has the following displacement field:

$$u(x, y, z, t) = u_0(x, y, t) + z\phi_x(x, y, t) - cz^3(\phi_x + \frac{\partial w}{\partial x}) \quad (3.14)$$

$$v(x, y, z, t) = v_0(x, y, t) + z\phi_y(x, y, t) - cz^3(\phi_y + \frac{\partial w}{\partial y}) \quad (3.15)$$

$$w(x, y, z, t) = w_0(x, y, t) \quad (3.16)$$

Where  $c = \frac{4}{3h^2}$ , which indicates that shear strain is non-applicable on the bottom and the top of the plate (see Figure 8c). The components of the strain displacement relations (equation 3.1) are:

$$\mathbf{u}(X, t) = [u_0 \quad v_0 \quad w_0 \quad \phi_x \quad \phi_y]^T \quad (3.17)$$

$$\boldsymbol{\varepsilon}(X, t) = [\varepsilon_{x0} \quad \varepsilon_{y0} \quad \gamma_{xy0} \quad X_x \quad X_y \quad X_{xy} \quad \gamma_{xz0} \quad \gamma_{yz0} \quad X_{xs} \quad X_{ys} \quad X_{xys} \quad \gamma_{xzs} \quad \gamma_{yzs}]^T \quad (3.18)$$

$$\mathbf{D} = \begin{bmatrix} \partial/\partial x & 0 & 0 & 0 & 0 \\ 0 & \partial/\partial y & 0 & 0 & 0 \\ \partial/\partial y & \partial/\partial x & 0 & 0 & 0 \\ 0 & 0 & 0 & \partial/\partial x & 0 \\ 0 & 0 & 0 & 0 & \partial/\partial y \\ 0 & 0 & 0 & \partial/\partial y & \partial/\partial x \\ 0 & 0 & \partial/\partial x & 1 & 0 \\ 0 & 0 & \partial/\partial y & 0 & 1 \\ 0 & 0 & c\partial^2/\partial x^2 & c\partial/\partial x & 0 \\ 0 & 0 & c\partial^2/\partial y^2 & 0 & c\partial/\partial y \\ 0 & 0 & 2c\partial^2/\partial x\partial y & c\partial/\partial y & c\partial/\partial x \\ 0 & 0 & 3c\partial/\partial x & 3c & 0 \\ 0 & 0 & 3c\partial/\partial y & 0 & 3c \end{bmatrix} \quad (3.19)$$

Where the curvature and shear strain caused by higher order terms are  $X_{xs}, X_{ys}, X_{xys}, \gamma_{xzs}$  and  $\gamma_{yzs}$ .

Three-dimensional elastic theory for plate is the general theory where no assumptions are needed. The strain displacement relations components consist of the following:

$$\mathbf{u}(X, t) = [u(x, t) \quad v(x, y) \quad w(x, t)]^T \quad (3.20)$$

$$\boldsymbol{\varepsilon} = [\varepsilon_{xx} \quad \varepsilon_{yy} \quad \varepsilon_{zz} \quad \gamma_{xy} \quad \gamma_{xz} \quad \gamma_{yz}]^T \quad (3.21)$$

$$\mathbf{D} = \begin{bmatrix} \partial/\partial x & 0 & 0 \\ 0 & \partial/\partial y & 0 \\ 0 & 0 & \partial/\partial z \\ \partial/\partial y & \partial/\partial x & 0 \\ \partial/\partial z & 0 & \partial/\partial x \\ 0 & \partial/\partial z & \partial/\partial y \end{bmatrix} \quad (3.22)$$

And the constitutive relations for linear elastic body can be written in a matrix for as:

$$\boldsymbol{\sigma} = \mathbf{H}\boldsymbol{\varepsilon} \quad (3.23)$$

And the components of equation (30) are as follow:

$$\boldsymbol{\sigma} = [\sigma_{xx} \quad \sigma_{yy} \quad \sigma_{zz} \quad \tau_{xy} \quad \tau_{xz} \quad \tau_{yz}]^T \quad (3.24)$$

$$\mathbf{H} = \frac{E(1-\nu)}{(1+\nu)(1-2\nu)} \begin{bmatrix} 1 & \frac{\nu}{1-\nu} & \frac{\nu}{1-\nu} & 0 & 0 & 0 \\ \frac{\nu}{1-\nu} & 1 & \frac{\nu}{1-\nu} & 0 & 0 & 0 \\ \frac{\nu}{1-\nu} & \frac{\nu}{1-\nu} & 1 & 0 & 0 & 0 \\ 0 & 0 & 0 & \frac{1-2\nu}{2(1-\nu)} & 0 & 0 \\ 0 & 0 & 0 & 0 & \frac{1-2\nu}{2(1-\nu)} & 0 \\ 0 & 0 & 0 & 0 & 0 & \frac{1-2\nu}{2(1-\nu)} \end{bmatrix} \quad (3.25)$$

The matrix  $\mathbf{H}$  indicates the elastic stiffness moduli for isentropic materials, and for FGM,  $\mathbf{H}$  is a function of the plate thickness,  $\mathbf{H}(z)$ .

### 3.2 General Assumptions and Configuration

For the solid plate with a rectangular shape having a, b and h as length, width and thickness, respectively, the following several assumptions are made in the FGM plate response formulation. These include constant Poisson's ratios ( $\nu$ ), elastic moduli that varies only in the transverse direction  $E(z)$  (across the thickness) based on the volume fractions (power, sigmoid and exponential laws), and various side-to-thickness ratios, so that typical

sample of thin-thick plates are included in this study. In addition, the panels are assumed to be have simply supported boundary condition on all the edges.

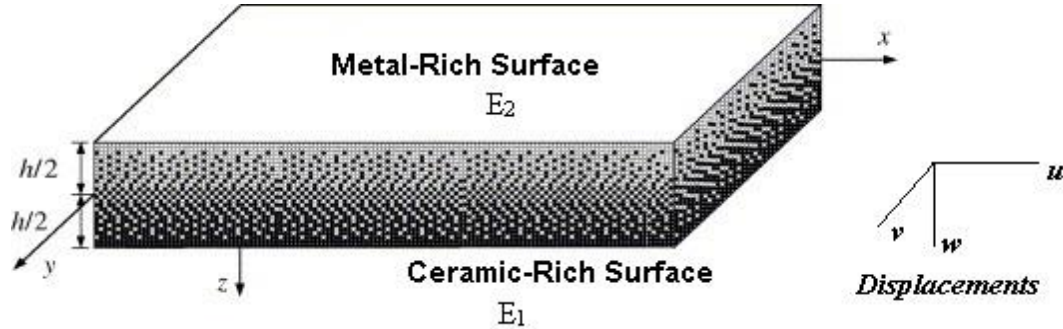


Figure 9: FGM plate geometric features

For the plate shown in Figure 9, the midplane (neutral surface) of the plate holds the origin point of Cartesian axes and the x-y axes, whereas the positive z axis points downward. As assumed before the moduli of elasticity are functions of the thickness and depend on volume fractions of the FGM plate. The volume fractions  $g_1, g_2$  and the corresponding material property  $P(z)$ , for instance, materials densities  $\rho$ , coefficients of thermal expansion  $\alpha$  or elasticity moduli  $E$ , for several FGM plate classifications that were mentioned before are as follow [2]:

1. Power law (P-FGM):

$$g(z) = \left(\frac{z+h/2}{h}\right)^p \quad (3.26)$$

$$P(z) = g(z)P_1 + [1 - g(z)]P_2 \quad (3.27)$$

2. Sigmoid law (S-FGM):

$$g_1(z) = 1 - \frac{1}{2} \left(\frac{h/2-z}{h/2}\right)^p \quad (3.28)$$

$$g_2(z) = \frac{1}{2} \left(\frac{h/2+z}{h/2}\right)^p \quad (3.29)$$

$$P_1(z) = g_1(z)P_1 + [1 - g_1(z)]P_2 \quad (3.30)$$

$$P_2(z) = g_2(z)P_1 + [1 - g_2(z)]P_2 \quad (3.31)$$

3. Exponential law (E-FGM):

$$P(z) = P_2 e^{\eta(z+0.5h)}, \quad \eta = \frac{1}{h} \ln \left( \frac{P_1}{P_2} \right) \quad (3.32)$$

Where subscript 1 and 2 in expressions of  $g$  and  $P$  refer to bottom ( $0 \leq z \leq h/2$ ) and top ( $-h/2 \leq z \leq 0$ ), respectively.

In this study, the FGM panel undergoes several types of lateral loads, once at a time. These loads, expanded by Fourier series expansion, have the following form:

$$q(x, y) = \sum \sum Q_{mn} \sin a_f x \sin b_f y \quad (3.33)$$

Where,

$$Q_{mn} = \iint q(x, y) \sin a_f x \sin b_f y \, dx dy, \quad a_f = \frac{m\pi}{a} \text{ and } b_f = \frac{n\pi}{b} \quad (3.34)$$

Those loads are either uniformly distributed load, line load (parallel to  $x$  or  $y$  axes), concentrated load, or sinusoidal distributed load. Having  $q_0$ ,  $L_{x,0}$ ,  $L_{y,0}$  and  $C$  are the intensities of each type of load,  $m$  and  $n$  are odd integers, then  $Q_{mn}$  for each type of force can be expressed as:

1. Uniformly distributed load, where  $q(x, y) = q_0 = \text{Constant}$  :

$$Q_{mn} = \frac{16q_0}{\pi^2 mn} \quad (3.35a)$$

2. Line Load (Parallel to  $y$ ,  $x = x_0$ ), where  $q(x, y) = L_{x,0} = \text{Constant}$ :

$$Q_{mn} = \frac{8L_{x,0}}{a\pi n} \sin \frac{m\pi x_0}{a} \quad (3.35b)$$

3. Line Load (Parallel to  $x$ ,  $y = y_0$ ), where  $q(x, y) = L_{y,0} = \text{Constant}$ :

$$Q_{mn} = \frac{8L_{y,0}}{b\pi m} \sin \frac{n\pi y_0}{b} \quad (3.35c)$$

4. Concentrated Load, where  $q(x, y) = C = \text{Constant}$ , applied on  $(x_0, y_0)$ :

$$Q_{mn} = \frac{4C}{ab} \sin \frac{m\pi x_0}{a} \sin \frac{n\pi y_0}{b} \quad (3.35d)$$

5. Sinusoidal Distributed Load, where  $q(x, y) = q_{11} \sin \frac{n\pi}{a} \sin \frac{m\pi}{b}$  :

$$\text{All elements of } Q_{mn} \text{ are zeros, except: } q_{11} = \text{constant} \quad (3.35e)$$

### 3.3 Classical Plate Theory (CPT)

#### 3.3.1 Governing Equation

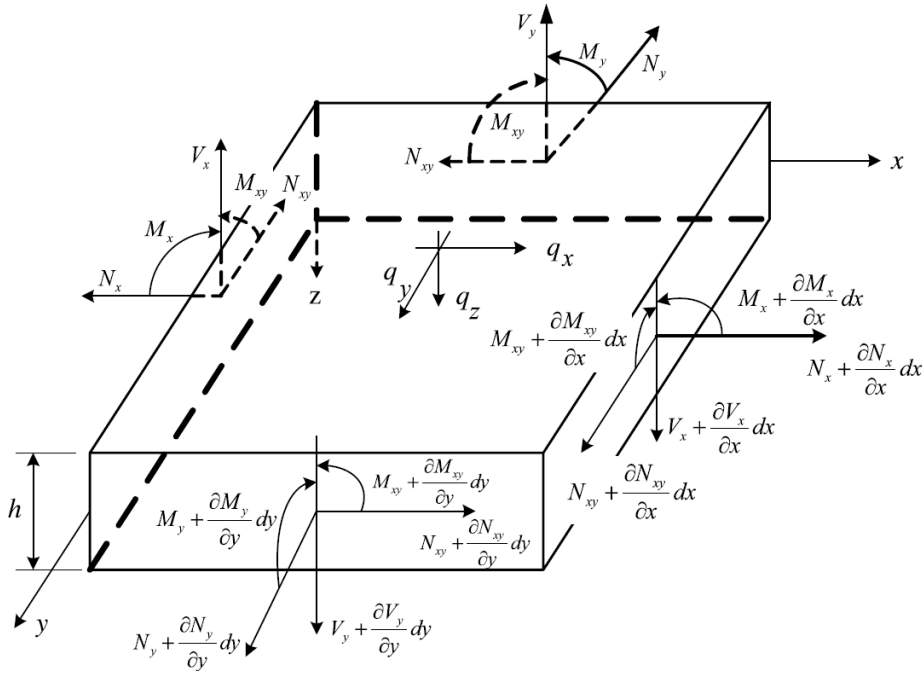


Figure 10: A small element of the plate subjected to forces and moments [2]

To develop the equations of equilibrium, for the case of the displacement field of small-displacement theory, the strain field can be written as (with the assumption of small deformation):

$$\varepsilon_x = \frac{\partial u}{\partial x} = \varepsilon_{x_0} - z \frac{\partial^2 w}{\partial x^2} \quad (3.36)$$

$$\varepsilon_y = \frac{\partial v}{\partial y} = \varepsilon_{y_0} - z \frac{\partial^2 w}{\partial y^2} \quad (3.37)$$

$$\gamma_{xy} = \frac{\partial u}{\partial y} + \frac{\partial v}{\partial x} = \gamma_{xy_0} - 2z \frac{\partial^2 w}{\partial x \partial y} \quad (3.38)$$

$$\varepsilon_z = \gamma_{xz} = \gamma_{yz} = 0 \quad (3.39)$$

According to the assumptions made, the plane stress-strain (constitutive) relations for the FGM plane are:

$$\sigma_x = \frac{E(z)}{1-\nu(z)^2} \left\{ \varepsilon_{x_0} + \nu(z) \varepsilon_{y_0} - z \left[ \frac{\partial^2 w}{\partial x^2} + \nu(z) \frac{\partial^2 w}{\partial y^2} \right] \right\} \quad (3.40)$$

$$\sigma_y = \frac{E(z)}{1-\nu(z)^2} \left\{ \varepsilon_{y_0} + \nu(z) \varepsilon_{x_0} - z \left[ \frac{\partial^2 w}{\partial y^2} + \nu(z) \frac{\partial^2 w}{\partial x^2} \right] \right\} \quad (3.41)$$

$$\tau_{xy} = \frac{E(z)}{1-\nu(z)^2} \left( \frac{1-\nu(z)}{2} \right) \left[ \gamma_{xy_0} - 2z \frac{\partial^2 w}{\partial x \partial y} \right] \quad (3.41)$$

Now, by integrating the stress-strain relations (equations (3.40) to (3.41)) through the thickness direction, the axial forces and the bending moments (see Figure 10) could be written in matrix form as:

$$\begin{Bmatrix} N_x \\ N_y \\ N_{xy} \end{Bmatrix} = \begin{bmatrix} A_{11} & A_{12} & 0 \\ A_{12} & A_{11} & 0 \\ 0 & 0 & A_{66} \end{bmatrix} \begin{Bmatrix} \varepsilon_{x_0} \\ \varepsilon_{y_0} \\ \gamma_{xy_0} \end{Bmatrix} + \begin{bmatrix} B_{11} & B_{12} & 0 \\ B_{12} & B_{11} & 0 \\ 0 & 0 & B_{66} \end{bmatrix} \begin{Bmatrix} -\frac{\partial^2 w}{\partial x^2} \\ -\frac{\partial^2 w}{\partial y^2} \\ -2\frac{\partial^2 w}{\partial x \partial y} \end{Bmatrix} \quad (3.43)$$

$$\begin{Bmatrix} M_x \\ M_y \\ M_{xy} \end{Bmatrix} = \begin{bmatrix} B_{11} & B_{12} & 0 \\ B_{12} & B_{11} & 0 \\ 0 & 0 & B_{66} \end{bmatrix} \begin{Bmatrix} \varepsilon_{x_0} \\ \varepsilon_{y_0} \\ \gamma_{xy_0} \end{Bmatrix} + \begin{bmatrix} C_{11} & C_{12} & 0 \\ C_{12} & C_{11} & 0 \\ 0 & 0 & C_{66} \end{bmatrix} \begin{Bmatrix} -\frac{\partial^2 w}{\partial x^2} \\ -\frac{\partial^2 w}{\partial y^2} \\ -2\frac{\partial^2 w}{\partial x \partial y} \end{Bmatrix} \quad (3.44)$$

Where  $A_{ij}$ ,  $B_{ij}$  and  $C_{ij}$  are stiffness coefficients of the panel.

Consider a small element formed from the plate, and undergoing distributed loads along x, y and z axes ( $q_x$ ,  $q_y$  and  $q_z$ ) with all those forces are shown in Figure 10. Let this element

be in equilibrium, then applying equilibrium equations in x, y and z directions along with some substitutions and simplifications, the equilibrium and compatibility equations can be expressed, respectively, as:

$$Q_{12} \frac{\partial^4 \phi}{\partial x^4} + 2(Q_{11} - Q_{66}) \frac{\partial^4 \phi}{\partial x^2 \partial y^2} + Q_{12} \frac{\partial^4 \phi}{\partial y^4} + S_{11} \frac{\partial^4 w}{\partial x^4} + 2(S_{12} + 2S_{66}) \frac{\partial^4 w}{\partial x^2 \partial y^2} + S_{11} \frac{\partial^4 w}{\partial y^4} = q_z(x, y) \quad (3.45)$$

$$P_{11} \frac{\partial^4 \phi}{\partial x^4} + (2P_{12} - P_{66}) \frac{\partial^4 \phi}{\partial x^2 \partial y^2} + P_{11} \frac{\partial^4 \phi}{\partial y^4} - Q_{12} \frac{\partial^4 w}{\partial x^4} - 2(Q_{11} + Q_{66}) \frac{\partial^4 w}{\partial x^2 \partial y^2} - Q_{12} \frac{\partial^4 w}{\partial y^4} = 0 \quad (3.46)$$

### 3.3.2 Series Solution of CPT

To get the solutions of FGM plate supported simply using Fourier expansions, first, consider the boundary conditions in case of simply supported panel, which are:

$$\begin{cases} w = 0 \\ M_x = 0 \end{cases} \quad \text{at } x = 0 \quad \text{and} \quad x = a \quad (3.47a)$$

$$\begin{cases} w = 0 \\ M_y = 0 \end{cases} \quad \text{at } y = 0 \quad \text{and} \quad y = b \quad (3.47b)$$

The unknowns stress function  $\phi(x, y)$  and the displacement  $w$  in equations (3.45) and (3.46) must be expanded using Fourier series expansion as follow (for  $0 \leq x \leq a$  and  $0 \leq y \leq b$ ):

$$w(x, y) = \sum_m \sum_n w_{mn} \sin \frac{m\pi x}{a} \sin \frac{n\pi y}{b} \quad (3.48)$$

$$\phi(x, y) = \sum_m \sum_n \phi_{mn} \sin \frac{m\pi x}{a} \sin \frac{n\pi y}{b} \quad (3.49)$$

Then, substitute the above equations into the equilibrium and compatibility equations and solve them simultaneously in order to obtain the following:

$$w_{mn} = \left( \frac{J}{JH + K^2} \right) q_{mn} \quad \text{and} \quad \phi_{mn} = \left( \frac{K}{JH + K^2} \right) q_{mn} \quad (3.50)$$



The expressions of H, J, and K can be found in reference [2].

For constant Poisson's ratio and modulus of elasticity depends on z direction only, we get the following values if  $A_{ij}$ ,  $B_{ij}$ ,  $C_{ij}$ ,  $P_{ij}$ ,  $Q_{ij}$  and  $S_{ij}$ :

$$A_{12} = \nu A_{11}, \quad B_{12} = \nu B_{11}, \quad C_{12} = \nu C_{11}, \quad (3.51a)$$

$$A_{66} = \left(\frac{1-\nu}{2}\right) A_{11}, \quad B_{66} = \left(\frac{1-\nu}{2}\right) B_{11}, \quad C_{66} = \left(\frac{1-\nu}{2}\right) C_{11} \quad (3.51b)$$

$$P_{12} = -\nu P_{11}, \quad P_{66} = -2(1+\nu)P_{11}, \quad Q_{12} = 0 \quad (3.51c)$$

$$Q_{66} = Q_{11}, \quad S_{12} = \nu S_{11}, \quad S_{66} = \frac{1-\nu}{2} S_{11} \quad (3.51d)$$

$$P_{11} = \frac{1}{(1-\nu^2)A_{11}}, \quad Q_{11} = -\frac{B_{11}}{A_{11}}, \quad S_{11} = B_{11}Q_{11} + C_{11} \quad (3.51e)$$

Accordingly, the expressions of H, J, and K, which appear in equations (3.50) becomes:

$$H = S_{11} \left[ \left(\frac{m\pi}{a}\right)^2 + \left(\frac{n\pi}{b}\right)^2 \right]^2, \quad J = P_{11} \left[ \left(\frac{m\pi}{a}\right)^2 + \left(\frac{n\pi}{b}\right)^2 \right]^2, \quad K = 0 \quad (3.52)$$

From the above equations, the deflection is:

$$w = \frac{1}{S_{11}} \sum_m \sum_n \frac{q_{mn}}{\left[ \left(\frac{m\pi}{a}\right)^2 + \left(\frac{n\pi}{b}\right)^2 \right]^2} \sin \frac{m\pi x}{a} \sin \frac{n\pi y}{b} \quad (3.53)$$

In the end, strains, stresses, axial forces and bending moments can be expressed as Fourier series solution for the FGM plate having  $\nu = \text{constant}$  and  $E = E(z)$  as follow:

$$\varepsilon_{x0} = \frac{Q_{11}}{S_{11}} \sum_m \sum_n \frac{q_{mn} \left(\frac{m\pi}{a}\right)^2}{\left[ \left(\frac{m\pi}{a}\right)^2 + \left(\frac{n\pi}{b}\right)^2 \right]^2} \sin \frac{m\pi x}{a} \sin \frac{n\pi y}{b} \quad (3.54a)$$

$$\varepsilon_{y0} = \frac{Q_{11}}{S_{11}} \sum_m \sum_n \frac{q_{mn} \left(\frac{n\pi}{b}\right)^2}{\left[ \left(\frac{m\pi}{a}\right)^2 + \left(\frac{n\pi}{b}\right)^2 \right]^2} \sin \frac{m\pi x}{a} \sin \frac{n\pi y}{b} \quad (3.54b)$$

$$\gamma_{xy0} = \frac{-2Q_{11}}{S_{11}} \sum_m \sum_n \frac{q_{mn} \left(\frac{m\pi}{a}\right) \left(\frac{n\pi}{b}\right)}{\left[ \left(\frac{m\pi}{a}\right)^2 + \left(\frac{n\pi}{b}\right)^2 \right]^2} \cos \frac{m\pi x}{a} \cos \frac{n\pi y}{b} \quad (3.54c)$$

$$\varepsilon_x = \frac{Q_{11}+z}{S_{11}} \sum_m \sum_n \frac{q_{mn} \left(\frac{m\pi}{a}\right)^2}{\left[\left(\frac{m\pi}{a}\right)^2 + \left(\frac{n\pi}{b}\right)^2\right]^2} \sin \frac{m\pi x}{a} \sin \frac{n\pi y}{b} \quad (3.54d)$$

$$\varepsilon_y = \frac{Q_{11}+z}{S_{11}} \sum_m \sum_n \frac{q_{mn} \left(\frac{n\pi}{b}\right)^2}{\left[\left(\frac{m\pi}{a}\right)^2 + \left(\frac{n\pi}{b}\right)^2\right]^2} \sin \frac{m\pi x}{a} \sin \frac{n\pi y}{b} \quad (3.54e)$$

$$\gamma_{xy} = \frac{-2(Q_{11}+z)}{S_{11}} \sum_m \sum_n \frac{q_{mn} \left(\frac{m\pi}{a}\right) \left(\frac{n\pi}{b}\right)}{\left[\left(\frac{m\pi}{a}\right)^2 + \left(\frac{n\pi}{b}\right)^2\right]^2} \cos \frac{m\pi x}{a} \cos \frac{n\pi y}{b} \quad (3.54f)$$

$$\sigma_x = \frac{E(z)}{(1-\nu^2)} \frac{(Q_{11}+z)}{S_{11}} \sum_m \sum_n q_{mn} \frac{\left(\frac{m\pi}{a}\right)^2 + \nu \left(\frac{n\pi}{b}\right)^2}{\left[\left(\frac{m\pi}{a}\right)^2 + \left(\frac{n\pi}{b}\right)^2\right]^2} \sin \frac{m\pi x}{a} \sin \frac{n\pi y}{b} \quad (3.55a)$$

$$\sigma_y = \frac{E(z)}{(1-\nu^2)} \frac{(Q_{11}+z)}{S_{11}} \sum_m \sum_n q_{mn} \frac{\left(\frac{n\pi}{b}\right)^2 + \nu \left(\frac{m\pi}{a}\right)^2}{\left[\left(\frac{m\pi}{a}\right)^2 + \left(\frac{n\pi}{b}\right)^2\right]^2} \sin \frac{m\pi x}{a} \sin \frac{n\pi y}{b} \quad (3.55b)$$

$$\tau_{xy} = \frac{-E(z)}{(1+\nu)} \frac{(Q_{11}+z)}{S_{11}} \sum_m \sum_n q_{mn} \frac{\left(\frac{m\pi}{a}\right) \left(\frac{n\pi}{b}\right)}{\left[\left(\frac{m\pi}{a}\right)^2 + \left(\frac{n\pi}{b}\right)^2\right]^2} \cos \frac{m\pi x}{a} \cos \frac{n\pi y}{b} \quad (3.55c)$$

$$N_x = N_y = N_{xy} = 0 \quad (3.56)$$

$$M_x = \sum_m \sum_n q_{mn} \frac{\left(\frac{m\pi}{a}\right)^2 + \nu \left(\frac{n\pi}{b}\right)^2}{\left[\left(\frac{m\pi}{a}\right)^2 + \left(\frac{n\pi}{b}\right)^2\right]^2} \sin \frac{m\pi x}{a} \sin \frac{n\pi y}{b} \quad (3.57a)$$

$$M_y = \sum_m \sum_n q_{mn} \frac{\left(\frac{n\pi}{b}\right)^2 + \nu \left(\frac{m\pi}{a}\right)^2}{\left[\left(\frac{m\pi}{a}\right)^2 + \left(\frac{n\pi}{b}\right)^2\right]^2} \sin \frac{m\pi x}{a} \sin \frac{n\pi y}{b} \quad (3.57b)$$

$$M_{xy} = \sum_m \sum_n q_{mn} \frac{(\nu-1) \left(\frac{m\pi}{a}\right) \left(\frac{n\pi}{b}\right)}{\left[\left(\frac{m\pi}{a}\right)^2 + \left(\frac{n\pi}{b}\right)^2\right]^2} \cos \frac{m\pi x}{a} \cos \frac{n\pi y}{b} \quad (3.57c)$$

The complete series solutions for a given volume fraction can be obtained by substituting the expression of Young's modulus corresponding to that volume fraction into equations of the coefficients  $A_{ij}$ ,  $B_{ij}$  and  $C_{ij}$  found in equations (14) from reference [2], then, by substituting those new values of  $A_{ij}$ ,  $B_{ij}$  and  $C_{ij}$  (after integration) into equations

(3.51e),  $P_{11}$ ,  $Q_{11}$  and  $S_{11}$  can be found in order to use them in equations (3.54) to (3.57) for analyzing the mechanical responses of FGM plates. Therefore, for power law function, P-FGM,  $P_{11}$ ,  $Q_{11}$  and  $S_{11}$  are:

$$P_{11} = \frac{p+1}{h(pE_2+E_1)} \quad (3.58a)$$

$$Q_{11} = \frac{-ph}{2(p+2)} \frac{(E_1-E_2)}{(pE_2+E_1)} \quad (3.58b)$$

$$S_{11} = \frac{h^3}{12(1-\nu^2)} \left[ E_2 + \frac{3(p^2+P+2)(E_1-E_2)}{(p+1)(p+2)(p+3)} - \frac{3p^2(E_1-E_2)^2}{(p+1)(p+2)^2(pE_2+E_1)} \right] \quad (3.58c)$$

For sigmoid functions, S-FGM:

$$P_{11} = \frac{2}{h(E_1+E_2)} \quad (3.59a)$$

$$Q_{11} = \frac{-h(E_1-E_2)(p^2+3p)}{4(E_1+E_2)(p+1)(p+2)} \quad (3.59b)$$

$$S_{11} = \frac{h^3}{8(1-\nu^2)} \left[ \frac{E_1+E_2}{3} - \frac{(E_1-E_2)^2(p^2+3p)^2}{4(E_1+E_2)(p+1)^2(p+2)^2} \right] \quad (3.59c)$$

Whereas for exponential function, E-FGM, they be written as:

$$P_{11} = \frac{1}{h} \frac{\ln(E_1/E_2)}{(E_1-E_2)} \quad (3.60a)$$

$$Q_{11} = \frac{h}{\ln(E_1/E_2)} - \frac{h(E_1+E_2)}{2(E_1-E_2)} \quad (3.60b)$$

$$S_{11} = \frac{h^3}{1-\nu^2} \left[ \frac{(E_1-E_2)^2 - E_1E_2[\ln(E_1/E_2)]^2}{[\ln(E_1/E_2)]^3(E_1-E_2)} \right] \quad (3.60c)$$

To demonstrate the use of the above equations to get the deflection, strain and stresses, an S-FGM plate stresses, strain and deflection are obtained by using equations (3.59b) and (3.59c) to find  $Q_{11}$  and  $S_{11}$ , which give:

$$Q_{11} = -\frac{5h(E_1/E_2-1)}{24(E_1/E_2+1)} \quad (3.61a)$$

$$S_{11} = \frac{h^3 E_2}{8(1-\nu^2)} \left[ \frac{E_1/E_2+1}{3} - \frac{25(E_1/E_2-1)^2}{144(E_1/E_2+1)} \right] \quad (3.61b)$$

For the case of a uniform load, and using Fourier expansion, with  $m, n = 1, 3, 5, \dots$ , then, from equations (3.54) to (3.57), deflection, strain and stresses can be found to be:

$$w = \frac{16q_0 b^4}{\pi^6} \frac{1}{S_{11}} \sum_m \sum_n \frac{1}{mn \left[ \left( \frac{mb}{a} \right)^2 + n^2 \right]^2} \sin \frac{m\pi x}{a} \sin \frac{n\pi y}{b} \quad (62)$$

$$\varepsilon_{xx} = \frac{16q_0 b^2}{\pi^4} \frac{Q_{11} + z}{S_{11}} \sum_m \sum_n \frac{\left( \frac{mb}{a} \right)^2}{mn \left[ \left( \frac{mb}{a} \right)^2 + n^2 \right]^2} \sin \frac{m\pi x}{a} \sin \frac{n\pi y}{b} \quad (3.63)$$

$$\sigma_{xx} = \frac{16q_0 b^2}{\pi^4} \frac{E(z)(Q_{11} + z)}{(1-\nu^2)S_{11}} \sum_m \sum_n \frac{\left( \frac{mb}{a} \right)^2 + \nu n^2}{mn \left[ \left( \frac{mb}{a} \right)^2 + n^2 \right]^2} \sin \frac{m\pi x}{a} \sin \frac{n\pi y}{b} \quad (3.64a)$$

$$\sigma_{yy} = \frac{16q_0 b^2}{\pi^4} \frac{E(z)(Q_{11} + z)}{(1-\nu^2)S_{11}} \sum_m \sum_n \frac{n^2 + \nu \left( \frac{mb}{a} \right)^2}{mn \left[ \left( \frac{mb}{a} \right)^2 + n^2 \right]^2} \sin \frac{m\pi x}{a} \sin \frac{n\pi y}{b} \quad (3.64b)$$

With  $Q_{11}$  and  $S_{11}$  values obtained from equations (3.61).

### 3.4 Third Order Shear Deformation Theory (TSDT)

#### 3.4.1 Governing Equations

Referring to equations (3.14) to (3.16), which shows the displacement field of the plate theory in the third order form, using Cartesian coordinates, where the origin is positioned in the plate center, and the deflection components on the axes of Cartesian system ( $x, y$  and  $z$ ) for this plate is described as  $u, v$  and  $w$ , which are functions of  $x, y$  and  $z$  coordinates, respectively along with  $t$  (time), the linear strains can be defined as:

$$\begin{Bmatrix} \varepsilon_{xx} \\ \varepsilon_{yy} \\ \gamma_{xy} \end{Bmatrix} = \begin{Bmatrix} \varepsilon_{xx}^{(0)} \\ \varepsilon_{yy}^{(0)} \\ \gamma_{xy}^{(0)} \end{Bmatrix} + z \begin{Bmatrix} \varepsilon_{xx}^{(1)} \\ \varepsilon_{yy}^{(1)} \\ \gamma_{xy}^{(1)} \end{Bmatrix} + z^3 \begin{Bmatrix} \varepsilon_{xx}^{(3)} \\ \varepsilon_{yy}^{(3)} \\ \gamma_{xy}^{(3)} \end{Bmatrix}, \quad \begin{Bmatrix} \gamma_{yz} \\ \gamma_{xz} \end{Bmatrix} = \begin{Bmatrix} \gamma_{yz}^{(0)} \\ \gamma_{xz}^{(0)} \end{Bmatrix} + z^2 \begin{Bmatrix} \gamma_{yz}^{(2)} \\ \gamma_{xz}^{(2)} \end{Bmatrix} \quad (3.65)$$

Where;

$$\begin{aligned}
\begin{Bmatrix} \varepsilon_{xx}^{(0)} \\ \varepsilon_{yy}^{(0)} \\ \gamma_{xy}^{(0)} \end{Bmatrix} &= \begin{Bmatrix} \frac{\partial u_0}{\partial x} \\ \frac{\partial u_0}{\partial y} \\ \frac{\partial u_0}{\partial y} + \frac{\partial v_0}{\partial x} \end{Bmatrix}, & \begin{Bmatrix} \varepsilon_{xx}^{(1)} \\ \varepsilon_{yy}^{(1)} \\ \gamma_{xy}^{(1)} \end{Bmatrix} &= \begin{Bmatrix} \frac{\partial \phi_x}{\partial x} \\ \frac{\partial \phi_y}{\partial y} \\ \frac{\partial \phi_x}{\partial y} + \frac{\partial \phi_y}{\partial x} \end{Bmatrix}, & \begin{Bmatrix} \varepsilon_{xx}^{(3)} \\ \varepsilon_{yy}^{(3)} \\ \gamma_{xy}^{(3)} \end{Bmatrix} &= \\
& & & & -c \begin{Bmatrix} \frac{\partial \phi_x}{\partial x} + \frac{\partial^2 w_0}{\partial x^2} \\ \frac{\partial \phi_y}{\partial y} + \frac{\partial^2 w_0}{\partial y^2} \\ \frac{\partial \phi_x}{\partial y} + \frac{\partial \phi_y}{\partial x} + 2 \frac{\partial^2 w_0}{\partial x \partial y} \end{Bmatrix} \\
\begin{Bmatrix} \gamma_{yz}^{(0)} \\ \gamma_{xz}^{(0)} \end{Bmatrix} &= \begin{Bmatrix} \phi_y + \frac{\partial w_0}{\partial y} \\ \phi_x + \frac{\partial w_0}{\partial x} \end{Bmatrix}, & \begin{Bmatrix} \gamma_{yz}^{(2)} \\ \gamma_{xz}^{(2)} \end{Bmatrix} &= -3c \begin{Bmatrix} \phi_y + \frac{\partial w_0}{\partial y} \\ \phi_x + \frac{\partial w_0}{\partial x} \end{Bmatrix}
\end{aligned} \tag{3.66}$$

Moreover, linear constitutive relations can be written as:

$$\begin{Bmatrix} \sigma_{xx} \\ \sigma_{yy} \\ \sigma_{yz} \\ \sigma_{xz} \\ \sigma_{xy} \end{Bmatrix} = \begin{bmatrix} Q_{11} & Q_{12} & 0 & 0 & 0 \\ Q_{12} & Q_{11} & 0 & 0 & 0 \\ 0 & 0 & Q_{44} & 0 & 0 \\ 0 & 0 & 0 & Q_{55} & 0 \\ 0 & 0 & 0 & 0 & Q_{66} \end{bmatrix} \left( \begin{Bmatrix} \varepsilon_{xx} \\ \varepsilon_{yy} \\ \gamma_{yz} \\ \gamma_{xz} \\ \gamma_{xy} \end{Bmatrix} - \begin{Bmatrix} 1 \\ 1 \\ 0 \\ 0 \\ 0 \end{Bmatrix} \alpha \Delta T \right) \tag{3.67}$$

Where,

$$Q_{11} = \frac{E(z)}{1-\nu^2}, \quad Q_{12} = \nu Q_{11}, \quad Q_{44} = Q_{55} = Q_{66} = \frac{E(z)}{2(1+\nu)} \tag{3.68}$$

$\Delta T$  is the change in temperature during stress-free state. Since  $Q_{ij}$  depends on the moduli of elasticity and thermal expansion coefficients which obey the volume fraction expressions, therefore, the values of  $Q_{ij}$  are function of  $z$ .

Now, the equations of motion constructed for TSDT can be written as:

$$\frac{\partial N_{xx}}{\partial x} + \frac{\partial N_{xy}}{\partial y} = I_0 \ddot{u}_0 + J_1 \ddot{\phi}_x - c I_3 \frac{\partial \ddot{w}_0}{\partial x}, \tag{3.69a}$$

$$\frac{\partial N_{xy}}{\partial x} + \frac{\partial N_{yy}}{\partial y} = I_0 \ddot{v}_0 + J_1 \ddot{\phi}_y - c I_3 \frac{\partial \ddot{w}_0}{\partial y} \tag{3.69b}$$

$$\frac{\partial \bar{Q}_x}{\partial x} + \frac{\partial \bar{Q}_y}{\partial y} + c \left( \frac{\partial^2 P_{xx}}{\partial x^2} + 2 \frac{\partial^2 P_{xy}}{\partial x \partial y} + \frac{\partial^2 P_{yy}}{\partial y^2} \right) + q = I_0 \ddot{w}_0 - c^2 \left( \frac{\partial^2 \dot{w}_0}{\partial x^2} + \frac{\partial^2 \dot{w}_0}{\partial y^2} \right) + c \left[ I_3 \left( \frac{\partial \dot{u}_0}{\partial x} + \frac{\partial \dot{v}_0}{\partial y} \right) + J_4 \left( \frac{\partial \ddot{\phi}_x}{\partial x} + \frac{\partial \ddot{\phi}_y}{\partial y} \right) \right] \quad (3.69c)$$

$$\frac{\partial \bar{M}_{xx}}{\partial x} + \frac{\partial \bar{M}_{xy}}{\partial y} - \bar{Q}_x = J_1 \dot{u}_0 + K_2 \ddot{\phi}_x - c J_4 \frac{\partial \dot{w}_0}{\partial x} \quad (3.69d)$$

$$\frac{\partial \bar{M}_{xy}}{\partial x} + \frac{\partial \bar{M}_{yy}}{\partial y} - \bar{Q}_y = J_1 \dot{v}_0 + K_2 \ddot{\phi}_y - c J_4 \frac{\partial \dot{w}_0}{\partial y} \quad (3.69e)$$

Where,

$$\bar{M}_{ab} = M_{ab} - c P_{ab}, \bar{Q}_a = Q_a - 3c R_a, \quad I_i = \int_{-h/2}^{h/2} p z^i dz \quad \text{for } (i = 0, 1, 2, \dots, 6)$$

$$J_i = I_i - c I_{i+2}, \quad K_2 = I_2 - 2c I_4 + c^2 I_6 \quad (3.70)$$

The in-plane total force and moment resultants which are  $N_{xx}, N_{yy}, N_{xy}, M_{xx}, M_{yy}$  and  $M_{xy}$ , respectively, are expressed as:

$$\begin{Bmatrix} N_{xx} \\ N_{yy} \\ N_{xy} \end{Bmatrix} = \int_{-h/2}^{h/2} \begin{Bmatrix} \sigma_{xx} \\ \sigma_{yy} \\ \sigma_{xy} \end{Bmatrix} dz, \quad \text{and} \quad \begin{Bmatrix} M_{xx} \\ M_{yy} \\ M_{xy} \end{Bmatrix} = \int_{-h/2}^{h/2} \begin{Bmatrix} \sigma_{xx} \\ \sigma_{yy} \\ \sigma_{xy} \end{Bmatrix} z dz \quad (3.71a)$$

And higher order stress resultants are:

$$\begin{Bmatrix} P_{xx} \\ P_{yy} \\ P_{xy} \end{Bmatrix} = \int_{-h/2}^{h/2} \begin{Bmatrix} \sigma_{xx} \\ \sigma_{yy} \\ \sigma_{xy} \end{Bmatrix} z^3 dz, \quad \text{and} \quad \begin{Bmatrix} R_x \\ R_y \end{Bmatrix} = \int_{-h/2}^{h/2} \begin{Bmatrix} \sigma_{yx} \\ \sigma_{xz} \end{Bmatrix} z^2 dz \quad (3.71b)$$

Furthermore, one can develop relations between stress resultants and strain as follow:

$$\begin{Bmatrix} \{N\} \\ \{M\} \\ \{P\} \end{Bmatrix} = \begin{bmatrix} \mathbf{A} & \mathbf{B} & \mathbf{E} \\ \mathbf{B} & \mathbf{D} & \mathbf{F} \\ \mathbf{E} & \mathbf{F} & \mathbf{H} \end{bmatrix} \begin{Bmatrix} \{\varepsilon^{(0)}\} \\ \{\varepsilon^{(1)}\} \\ \{\varepsilon^{(3)}\} \end{Bmatrix} - \begin{Bmatrix} \{N^T\} \\ \{M^T\} \\ \{P^T\} \end{Bmatrix} \quad (3.72)$$

Where each **Bold** litter, like **A**, above actually describes a matrix. And thermal forces and moments are defined as follow:

$$\{N^T\} = \int_{-h/2}^{h/2} \{\beta\} \Delta T dz, \quad (3.73a)$$

$$\{M^T\} = \int_{-h/2}^{h/2} \{\beta\} \Delta T z dz, \quad (3.73b)$$

$$\{P^T\} = \int_{-h/2}^{h/2} \{\beta\} \Delta T z^3 dz \quad (3.73c)$$

Where  $\{\beta\}$  is a vector related to the thermal expansion coefficient as:

$$\{\beta\} = [Q]\{\alpha\} = \begin{Bmatrix} (Q_{11} + Q_{12})\alpha \\ (Q_{12} + Q_{22})\alpha \\ 0 \end{Bmatrix} \quad (3.74)$$

The elements of matrices **A**, **D**, **F**, **B**, **E** and **H**, which are  $A_{ij}$ ,  $D_{ij}$ , and  $F_{ij}$  for  $(i, j = 1, 2, 4, 5, 6)$ , while  $B_{ij}$ ,  $E_{ij}$  and  $H_{ij}$  for  $(i, j = 1, 2, 6)$ , are expressed in a compact form as follow:

$$(A_{ij}, B_{ij}, D_{ij}, E_{ij}, F_{ij}, H_{ij}) = \int_{-h/2}^{h/2} Q_{ij}(1, z, z^2, z^3, z^4, z^6) dz \quad (3.75)$$

Equations (3.69) can be solved for the unknown displacements using a multitude of methods. These techniques can be classified into two categories. First, methods which lead to weak solutions (satisfying some of the boundary conditions), such as, Legendre polynomial expansions. Second, methods lead to strong solutions (satisfying all boundary conditions), like Navier's solutions, which employs a Fourier series expansion of the unknowns.

### 3.4.2 Series Solutions (The Navier's Solutions)

The following boundary conditions are applied for simply supported panel, and can be applied to the equations of motion, equations (3.69):

$$\begin{aligned} u_0(x, 0, t) = 0, \quad u_0(x, b, t) = 0, \quad v_0(0, y, t) = 0, \quad v_0(a, y, t) = 0, \\ w_0(x, b, t) = 0, \quad w_0(0, y, t) = 0, \quad w_0(a, y, t) = 0, \quad w_0(x, 0, t) = 0, \\ \phi_x(x, b, t) = 0, \quad \phi_y(0, y, t) = 0, \quad \phi_y(a, y, t) = 0, \quad \phi_x(x, 0, t) = 0, \end{aligned}$$

$$\begin{aligned}
N_{xx}(0, y, t) = 0, \quad N_{xx}(a, y, t) = 0, \quad N_{yy}(x, 0, t) = 0, \quad N_{yy}(x, b, t) = 0, \\
\bar{M}_{xx}(a, y, t) = 0, \quad \bar{M}_{yy}(x, 0, t) = 0, \quad \bar{M}_{yy}(x, b, t) = 0, \quad \bar{M}_{xx}(0, y, t) = 0,
\end{aligned} \tag{3.76}$$

Where the following Fourier expansions can be applied:

$$u_0(x, y, t) = \sum_{n=1}^{\infty} \sum_{m=1}^{\infty} U_{mn}(t) \cos(a_f x) \sin(b_f y) \tag{3.77a}$$

$$v_0(x, y, t) = \sum_{n=1}^{\infty} \sum_{m=1}^{\infty} V_{mn}(t) \sin(a_f x) \cos(b_f y) \tag{3.77b}$$

$$w_0(x, y, t) = \sum_{n=1}^{\infty} \sum_{m=1}^{\infty} W_{mn}(t) \sin(a_f x) \sin(b_f y) \tag{3.77c}$$

$$\phi_x(x, y, t) = \sum_{n=1}^{\infty} \sum_{m=1}^{\infty} X_{mn}(t) \cos(a_f x) \sin(b_f y) \tag{3.77d}$$

$$\phi_y(x, y, t) = \sum_{n=1}^{\infty} \sum_{m=1}^{\infty} Y_{mn}(t) \sin(a_f x) \cos(b_f y) \tag{3.77e}$$

Where;  $a_f = \frac{m\pi}{a}$  and  $b_f = \frac{n\pi}{b}$ .

By substituting equations (3.77) into the equations of motion and expand them properly, the following system of equations can be obtained:

$$\begin{aligned}
\begin{bmatrix} \hat{S}_{11} & \hat{S}_{12} & \hat{S}_{13} & \hat{S}_{14} & \hat{S}_{15} \\ \hat{S}_{12} & \hat{S}_{22} & \hat{S}_{23} & \hat{S}_{24} & \hat{S}_{25} \\ \hat{S}_{13} & \hat{S}_{23} & \hat{S}_{33} & \hat{S}_{34} & \hat{S}_{35} \\ \hat{S}_{14} & \hat{S}_{24} & \hat{S}_{34} & \hat{S}_{44} & \hat{S}_{45} \\ \hat{S}_{15} & \hat{S}_{25} & \hat{S}_{35} & \hat{S}_{45} & \hat{S}_{55} \end{bmatrix} \begin{Bmatrix} U_{mn} \\ V_{mn} \\ W_{mn} \\ X_{mn} \\ Y_{mn} \end{Bmatrix} + \begin{bmatrix} \hat{m}_{11} & 0 & 0 & 0 & 0 \\ 0 & \hat{m}_{22} & 0 & 0 & 0 \\ 0 & 0 & \hat{m}_{33} & \hat{m}_{34} & \hat{m}_{35} \\ 0 & 0 & \hat{m}_{34} & \hat{m}_{44} & 0 \\ 0 & 0 & \hat{m}_{35} & 0 & \hat{m}_{55} \end{bmatrix} \begin{Bmatrix} \ddot{U}_{mn} \\ \ddot{V}_{mn} \\ \ddot{W}_{mn} \\ \ddot{X}_{mn} \\ \ddot{Y}_{mn} \end{Bmatrix} = \\
\begin{Bmatrix} 0 \\ 0 \\ Q_{mn} \\ 0 \\ 0 \end{Bmatrix} - \begin{Bmatrix} a_f N_{1mn}^T \\ b_f N_{2mn}^T \\ 0 \\ a_f M_{1mn}^T \\ b_f M_{2mn}^T \end{Bmatrix} \tag{3.78}
\end{aligned}$$

Where the matrix  $\hat{S}_{ij}$  and  $\hat{m}_{ij}$  can be written as follow,



$$\begin{aligned}
\hat{s}_{11} &= A_{11}a_f^2 + A_{66}b_f^2, \quad \hat{s}_{12} = (A_{12} + A_{66})a_fb_f, \\
\hat{s}_{13} &= -c[E_{11}a_f^2 + (E_{12} + 2E_{66})b_f^2]a_f, \quad \hat{s}_{14} = \hat{B}_{11}a_f^2 + \hat{B}_{66}b_f^2, \\
\hat{s}_{15} &= (\hat{B}_{12} + \hat{B}_{66})a_fb_f, \\
\hat{s}_{22} &= A_{66}a_f^2 + A_{22}b_f^2, \quad \hat{s}_{23} = -c[E_{22}b_f^2 + (E_{12} + 2E_{66})a_f^2]b_f, \\
\hat{s}_{24} &= \hat{s}_{15}, \quad \hat{s}_{25} = \hat{B}_{66}a_f^2 + \hat{B}_{22}b_f^2 \\
\hat{s}_{33} &= \bar{A}_{55}a_f^2 + \bar{A}_{44}b_f^2 + c[H_{11}a_f^4 + 2(H_{12} + 2H_{66})a_f^2b_f^2 + H_{22}b_f^4], \\
\hat{s}_{34} &= \bar{A}_{55}a_fb_f - c[\hat{F}_{11}a_f^3 + (\hat{F}_{12} + 2\hat{F}_{66})a_fb_f^2], \\
\hat{s}_{35} &= \bar{A}_{44}b_fb_f - c[\hat{F}_{22}b_f^3 + (\hat{F}_{12} + 2\hat{F}_{66})a_f^2b_f], \\
\hat{s}_{44} &= \bar{A}_{55} + \bar{D}_{11}a_f^2 + \bar{D}_{66}b_f^2, \quad \hat{s}_{45} = (\bar{D}_{12} + \bar{D}_{66})a_fb_f, \\
\hat{s}_{55} &= \bar{A}_{44} + \bar{D}_{66}a_f^2 + \bar{D}_{22}b_f^2 \tag{3.79}
\end{aligned}$$

$$\begin{aligned}
\hat{m}_{11} &= \hat{m}_{22} = I_0, \quad \hat{m}_{33} = I_0 + c^2I_6(a_f^2 + b_f^2), \quad \hat{m}_{34} = -cJ_4a_fb_f \\
\hat{m}_{35} &= -cJ_4b_fb_f, \quad \hat{m}_{44} = \hat{m}_{55} = K_2 \tag{3.80}
\end{aligned}$$

$$\hat{A}_{ij} = A_{ij} - cD_{ij}, \quad \hat{B}_{ij} = B_{ij} - cE_{ij}, \quad (i,j = 1,2,3) \tag{3.81a}$$

$$\hat{D}_{ij} = D_{ij} - cF_{ij}, \quad \hat{F}_{ij} = F_{ij} - cH_{ij} \quad (i,j = 1,2,3) \tag{3.81b}$$

$$\bar{A}_{ij} = \hat{A}_{ij} - c\hat{D}_{ij} = A_{ij} - 2cD_{ij} + c^2F_{ij} \quad (i,j = 1,2,3) \tag{3.81c}$$

$$\bar{D}_{ij} = \hat{D}_{ij} - c\hat{F}_{ij} = D_{ij} - 2cF_{ij} + c^2H_{ij} \quad (i,j = 1,2,3) \tag{3.81d}$$

$$\bar{A}_{ij} = \hat{A}_{ij} - 3c\hat{D}_{ij} = A_{ij} - 6cD_{ij} + 9c^2F_{ij} \quad (i,j = 4,5) \tag{3.81e}$$

The above equations can be specialized to solve both static problems (deformation and stresses), as well as dynamic problems such as free dynamics (natural resonance frequencies and mode shapes) for classes of FG plates. These results do not exist for thick plates of two of the FGM types considered in this work, which are S-FGM and E-FGM. For gaining these promising outputs, a series of comprehensive and adaptive MATLAB

codes were written, such that they utilize core codes, which act as user-defined function, and then call them by multiple running programs (M-Script files), for simulating static behaviors using both CPT and TSDT, along with obtaining the free responses of all three classes of functionally graded plates.

## CHAPTER 4

### NUMERICAL RESULTS AND DISCUSSIONS

#### 4.1 Validation of The Model

In order to validate the mathematical model of the third order theory of shear distortion (TSDT) provided previously, a comparative study with results obtained by Mechab et al. [28] would be performed. First of all, for the sake of benchmarking for both static and dynamic behaviors, the plate specifications from [28] are implemented, which are clarified in Table 2, noticing that Poisson's ratios are constant. Moreover, since power law is most commonly used in the literature of FGM plates, the mentioned comparison is for P-FGM plate.

Table 2: FGM plate Material properties

Specifications	Top Surface:	Bottom Surface:
	Aluminum (Metal)	Alumina (Ceramic)
Young's Modulus (GPa)	70	380
Mass Density ( $kg/m^3$ )	2707	3800

### 4.1.1 Validating Model of Static Responses

For comparison purposes, a problem that was presented in earlier literature; namely [6] and [28], will be used here. The problem consists of a square plate ( $a=b=1$  m) subjected to a sinusoidal distributed load with an intensity of  $100 \text{ kN/m}^2$ . The plate is moderately thick with  $a/h = 10$ . Static response is presented in the form of non-dimensional maximum displacement at plate center, defined as:

$$\tilde{w} = \frac{10h^3 E_c}{a^4 q_0} w\left(\frac{a}{2}, \frac{b}{2}\right) \quad (4.1)$$

Where  $a$  and  $b$  are the side dimensions of the square plate,  $h$  denotes to the plate's depth,  $E_c$  is the elasticity modulus of the ceramic surface and  $q_0$  refers to the load's intensity. The Following table (table 3) illustrate how accurate is the present model compared to a model used in the literature, which used a four-variable model.

Table 3 insures that the proposed model generates preside outcomes for the plate deflection. Therefore, it be inferred that using either the present model, which includes five unknowns, or the model proposed by Mechab et al, which is a reduced version model with four unknown variables, would actually end up with precise results.

**Table 3: Comparing Dimensionless Deflections between the present model and Mechab et al. [28] model for a P-FGM plate**

Power indices	Dimensionless Deflection ( $\tilde{w}$ )			Percentage Difference between Present & Mechab et al.
	Zenkour [6]	Mechab et al. [28]	Present Model (TSDT)	
0 (Ceramic)	0.2960	0.2961	0.2961	0.000
1	0.5889	0.5889	0.5890	0.017
2	0.7573	0.7571	0.7573	0.026
5	0.9118	0.9112	0.9114	0.022
6	0.9356	0.9350	0.9351	0.011
9	0.9925	0.9921	0.9921	0.000
10	1.0089	1.0086	1.0087	0.010

#### 4.1.2 Validating Model of Dynamic Responses

For the dynamic behavior, comparison is based on the lowest non-dimensional natural frequency of the model, generally corresponding to the first mode ( $m=n=1$ ). This is defined as:

$$\tilde{\omega} = \frac{\omega b^2}{h} \sqrt{\frac{Q_0}{E_0}} \quad (4.2)$$

Where  $\omega$  represents the fundamental natural frequency,  $E_0 = 1 \text{ GPa}$  and  $Q_0 = 1 \text{ kg/m}^3$ .

According to the data comparison in Table 4, free vibration analysis is suited with both models, which are the present TSDT and the four-variable model. In fact, the reduced model tends to deviate little bit more from the HSDT compared to the five variables Model. Therefore, it might little bit more accurate if TSDT is implemented for investigating the free vibration results of an FGM plate, particularly for higher power indices, although using the reduced model would still give tremendous accuracy.

**Table 4: Comparative study between the present TSDT, Model II for Mechab et al. [28] and HSDT, for fundamental frequencies parameters of a P-FGM square plate.**

Power indices	Mode	Frequency Parameter ( $\tilde{\omega}$ )			Percentage Difference	
		Mechab et al. [28]		Present Model (TSDT)	Model II Vs. HSDT	(TSDT) Vs. HSDT
		Model II	HSDT			
1	1	1.3969	1.3969	1.3967	0.000	0.014
	2	7.2460	7.2394	7.2374	0.091	0.028
	3	12.226	12.225	12.2139	0.008	0.091
	4	53.210	53.252	53.1271	0.079	0.235
5	1	1.1908	1.1907	1.1909	0.008	0.017
	2	5.6544	5.6409	5.6399	0.239	0.018
	3	9.5080	9.5089	9.4976	0.009	0.119
	4	36.803	36.725	36.7394	0.212	0.039
10	1	1.1492	1.1491	1.1497	0.009	0.052
	2	5.1537	5.1462	5.1482	0.146	0.039
	3	8.6849	8.6847	8.6841	0.002	0.007
	4	33.4756	33.4397	33.4678	0.107	0.084

## 4.2 Parametric Study

After making sure that the present model, which is a five-variables model based on the third order form shear defamation theories of displacement field of plates, gives precise results and reliable outcomes, this section would discuss how an FGM plate responses to certain changes. The functionally graded plate is observed for 2 mechanical scenarios, namely, static and dynamic situations. In the static part, a certain static load is deployed on the top surface of the plate for considering the plates static characteristics. On the other hand, dynamics of that FG plate is put under consideration for free vibration responses.

### 4.2.1 Static Responses of Classes of FGM Panels

In this part, a detailed investigation regarding how a ceramic-metal plate respond statically when it is supported simply on all of its edges. The proposed composite plate is made of two common ingredients, Alumina as the ceramic part, while aluminum as the metal part, see Table 2 for the properties of those materials. In each parametric study, the plate would either has a square shape with each side length is equal to one meter long with the plate's thickness is one of the parameters under the study's consideration, or the plate thickness would be fixed to a thick value ( $b/h = 4$ ), while one of the plate's side length, which is  $a$ , varies, to investigate the cost of varying the aspect ratios on the static responses.

#### 4.2.1.1 Effects of Varying Material Gradient (Power Indices)

Consider a plate manufactured from functionally gradient materials, with simple supports around its edges. A uniformly distributed force is deployed on that plate with an intensity equals to 100 kilo Newtons per square meter. First, the response of changing



side length-to-thickness ratios on the plate's maximum deflection along with varying the power exponents is studied. Then, the influence for enlarging the plate's aspect ratio ( $a/b$ ) on the maximum deflection for a fixed thickness ratio ( $a/h = 4$ ) is considered.

The plate's response for various thickness ratios is shown on Figure 11, which reflects the influence of changing the material concentration throughout the thickness direction for both methods of manufacturing an FG plate (Power and Sigmoid). The interesting relationship of power and sigmoid laws can be inferred from the results. In both laws, raising the power index, which means the plates tend to be more ductile and have metal-like behavior, leads to higher deflections.

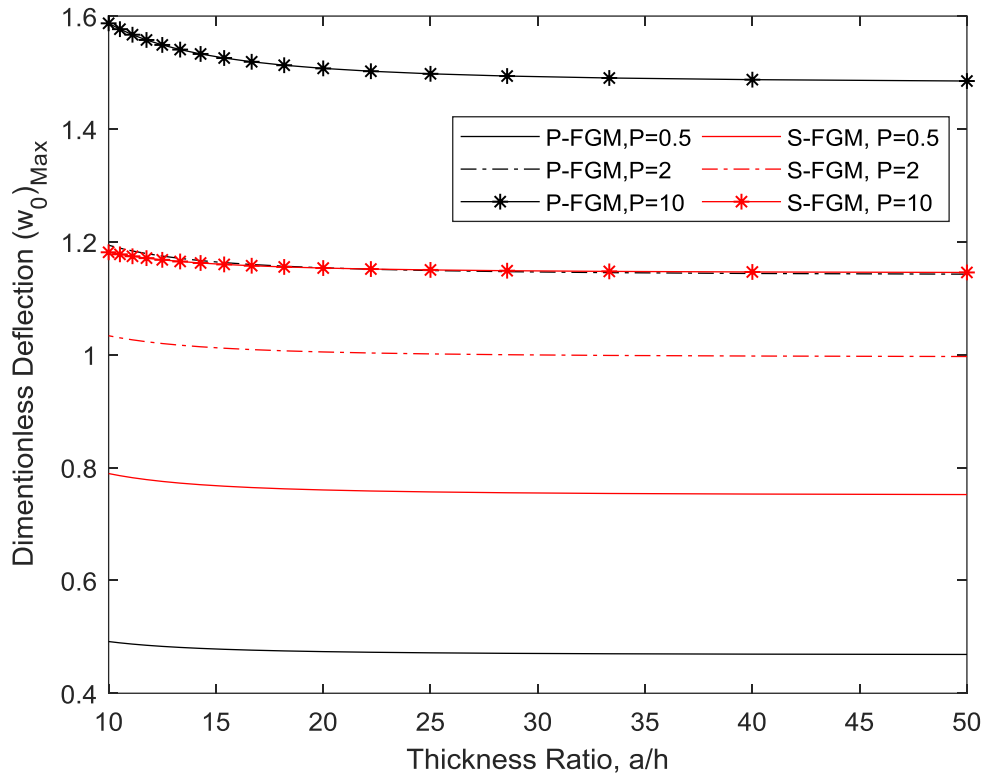


**Figure 11: Effects of varying power indices and thickness ratios on the plate's maximum deflection on P-FGM and S-FGM**

However, when power and sigmoid are under comparison, their corresponding natures tend to affect the plate's behaviors differently. For power indices greater than 1, the figure shows that S-FGM would result in less deflection, while the power volume distribution deflects higher. This relation is completely opposite when power indices are less than 1 for both laws.

This behavior can be best explained from Figures 4, 5 and 6, in the introduction part. To know why they behave like that, it is important to get back to the primary purpose of having two separated kinds of manufacturing methods, P- and S-, although they are basically power functions, with S- having 2 power-law volume fractions describe the material gradient in the top and the bottom part separately, instead of 1 function, in P-FGM, that describe the volume fraction in the whole plate thickness. For the case of power distribution with P greater than one, material properties change dramatically near the bottom surface. In other words, for the current case study where the metal constituent is located on the top part, and the ceramic is on the bottom, the plate tends to act more like a metal plate, which means more ductility and higher deflection, compared to S-FGM, which is designed to lower that sudden rate of change in material gradient to ensure smooth transition between metal to ceramic. When P is between zero and 1, the above relations is opposed, and the P-FGM plate tends to act more like a ceramic plate resulting in a stiffer panel compared to the S-FGM.

Figure 12, on the other hand, shows the effect of aspect ratio on the plate's maximum deflection, for thick FGM panels that have various power indices values. For high aspect ratios, around  $a/b > 4$ , that is for longer thick panels, the difference between P-FG and S-FG becomes negligible. Moreover, the same response of higher deflection associated

with P-FGM compared to S-FGM for  $P > 1$  is observed for low aspect ratios of thick panels.

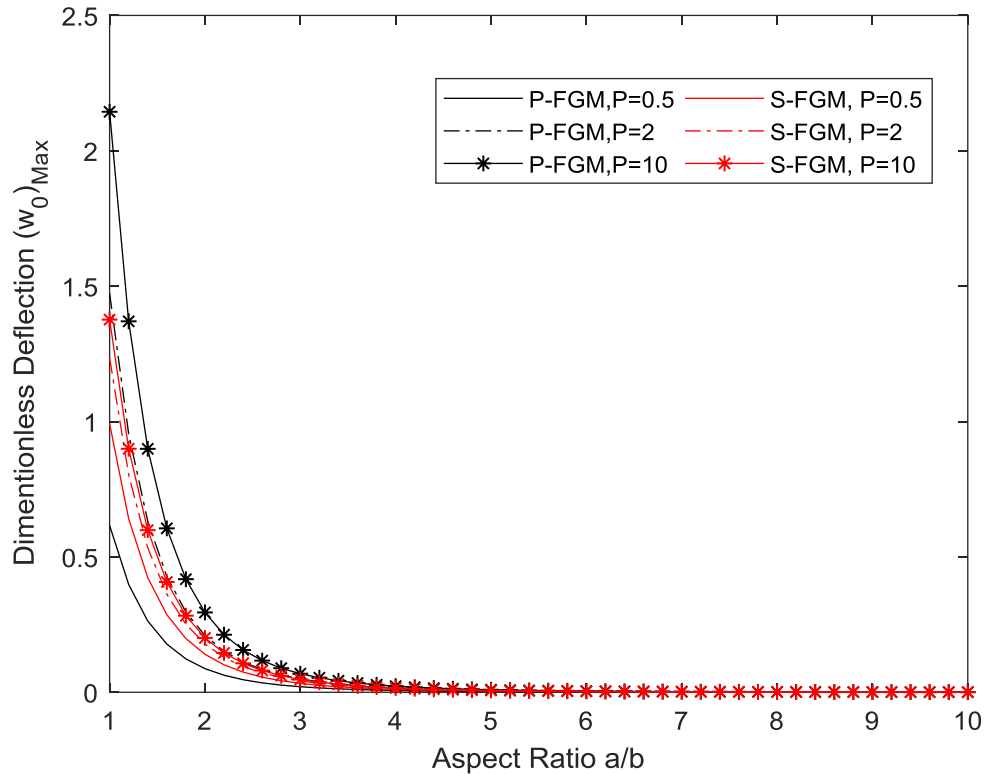


Figure 12: Effects of varying power indices and aspect ratios on the plate's maximum deflection on P-FGM and S-FGM

#### 4.2.1.2 Effect of Varying Modulus of Elasticity Ratio

Consider the same conditions and material specifications as in the first parametric study of the effect of changing the material power indices. On the current section, another class of parametric study is done for noticing how shifting between stiffness ratios of the surfaces ingredients affects the static responses of various types of FGM and comparing between those types' responses. Note that power indices of power and sigmoid plates are equal to

2, and the force applied on them is again in a uniformly distributed form, with an intensity equal to 100 kN.

Figure 13 represents the consequences of implementing different ratios of elastic modulus for a certain FGM plate for different thickness ratios, while Figure 14 shows results corresponding to various aspect ratios and a fixed thickness ratio. This implement that different prospective observed reactions are discussed. In general, each kind of the provided volume fraction gradients shows the same tendency of increasing the maximum deflection with the rise of Young's modulus ratios, regardless of how thick or long is the panel. This is obvious, since an increase in the shown ratio  $E_1/E_2$  means that the plate would have greater percentage of metal in it, i.e. higher ductility. However, for long thick panels, aspect ratios almost greater than 4, the effect of increasing  $E_1/E_2$  ratio is so small that can be neglected. Moreover, the plots show that for thin plates (higher values of  $a/h$  ratios) maximum deflections would be almost constant for each  $E_1/E_2$ .

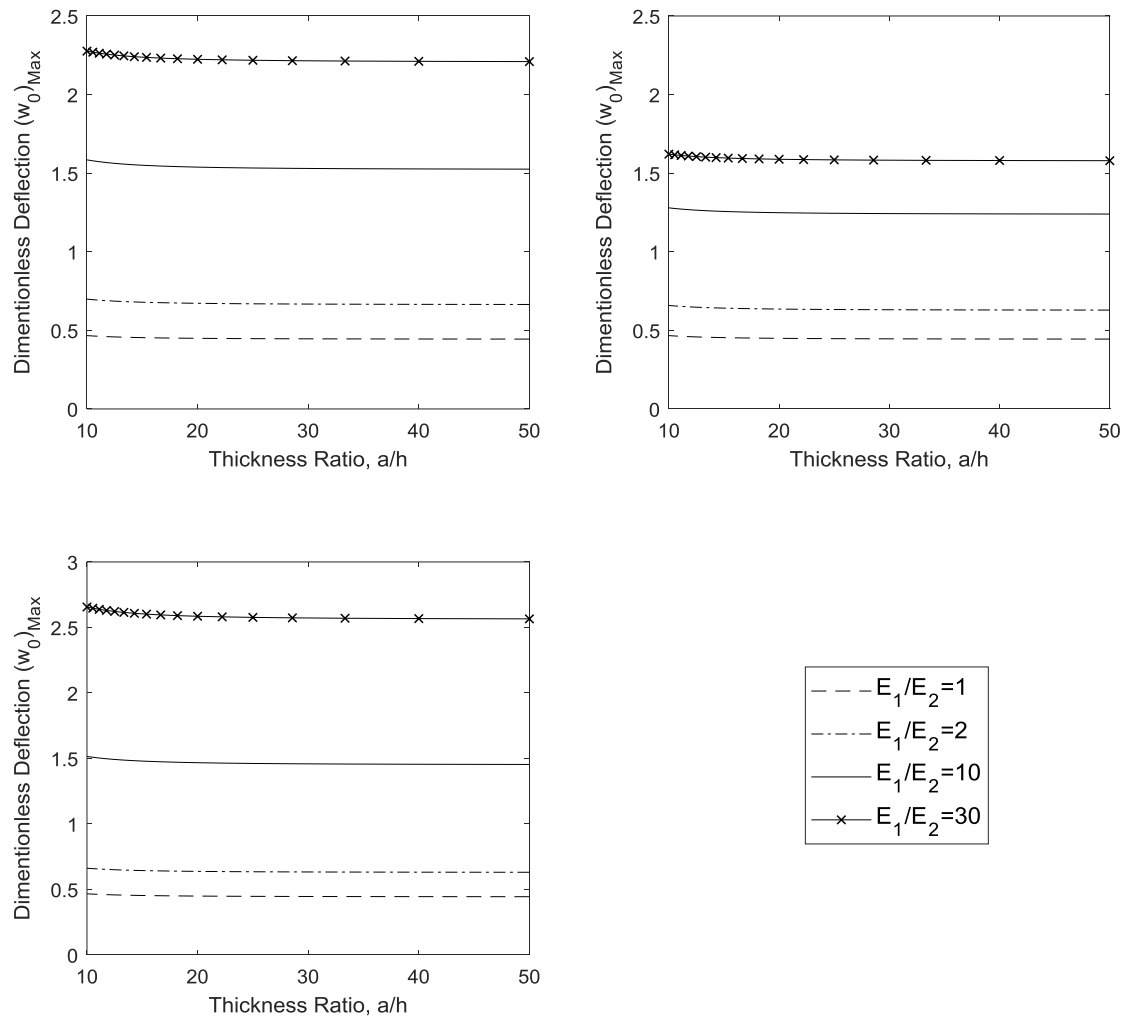


**Figure 13: Effects of varying Young's modulus ratios and thickness ratios on the plate's maximum deflection for a) P-FGM, b) S-FGM, and c) E-FGM, from top left to bottom, respectively.**

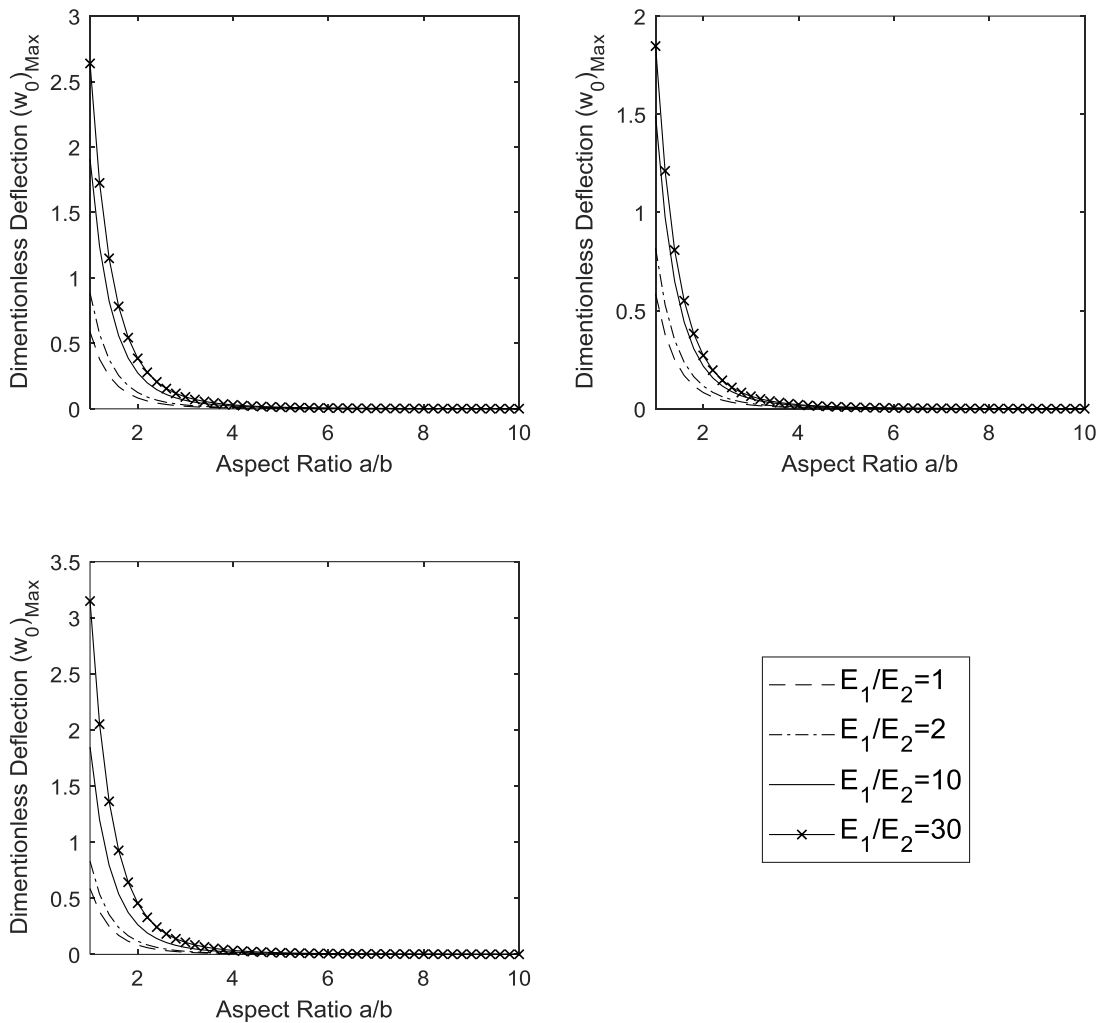


**Figure 14: Effects of varying Young's modulus ratios and aspect ratios on the plate's maximum deflection for P-  
a) FGM, b) S-FGM, and c) E-FGM from top left to bottom, respectively.**

To differentiate between the consequences of changing elastic moduli ratios for each volume gradient on the FGM Plate, Figures 15 and 16 signifies these effects with the influence of both factors of changing thickness and aspect ratios, respectively. As seen, in general, for higher values of  $E_1/E_2$ , which mean lower stiffness, the sigmoid law results in the lowest deflections because the way that the S-FGM is designed is to ensure gradual

change between properties near the surfaces, while E- shows stiffer behavior than P-. These differences tend to become negligible when  $E_1/E_2$  is closer to 1, specially for sigmoid and exponential laws. Moreover, a closer look at these figures shows that the effect of varying aspect ratios is more significant compared to increasing or decreasing thickness ratios. For instance, there is a slight change in the maximum deflection when the thickness ratio of a square P-FGM plate with  $E_1/E_2 = 10$  increase, compared to the steep drop in the maximum deflection happened for a thick power plate with the same elastic ratio, when the aspect ratio increases.

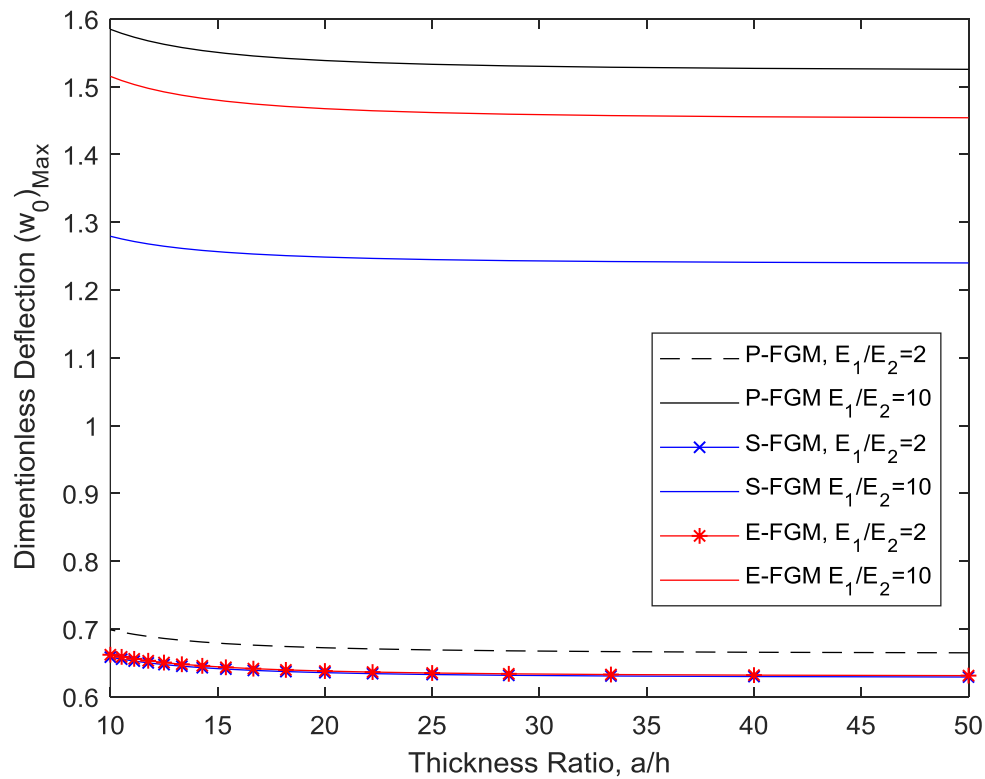


**Figure 15: Comparing the effects of varying Young's modulus ratios and thickness ratios on the plate's maximum deflection between P-FGM, S-FGM and E-FGM**

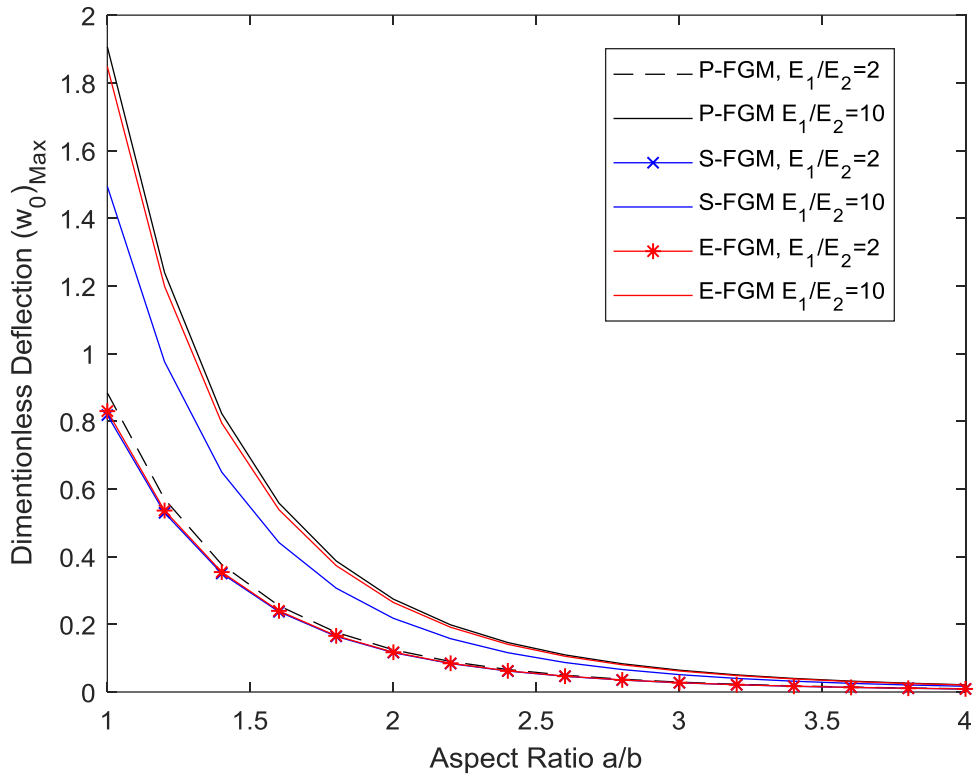


**Figure 16: Comparing the effects of varying Young's modulus ratios and aspect ratios on the plate's maximum deflection between P-FGM, S-FGM and E-FGM**

### 4.2.1.3 Responses for Different Static Loading Cases

Now, for studying the effects of different types static loading applied on thick, thin, square or rectangular panels, Figures 17 and 18 illustrate the influence of a concentrated force and a sinusoidal distributed force pressing on panels with either a fixed aspect ratio and variable thickness ratios, or vice-versa, respectively. For the loadings, the load value for the concentrated force, and the intensity of the sinusoidal load are 100 kilo Newton and 100 kilo Newton per meter squared, respectively. First, the panel is assumed to be square with an area of  $1 m^2$ , and the power indices used in P- and S- are equal to 5. Then the same panel is assumed to have a fixed thickness of 25 cm with variable side lengths. Both results



show panels with thickness-wise volume distribution and power function have the highest ductility, with higher aspect ratios leading to constant deflection predictions, which confirm the pervious findings, though two different types of loading have been investigated. Furthermore, Figure 17 shows that P-FGM always has higher maximum deflection, while the sigmoid has the least deflection for thick plates (around thickness ratios less than 8), but for thinner panels, E-FGM has the lowest bending.

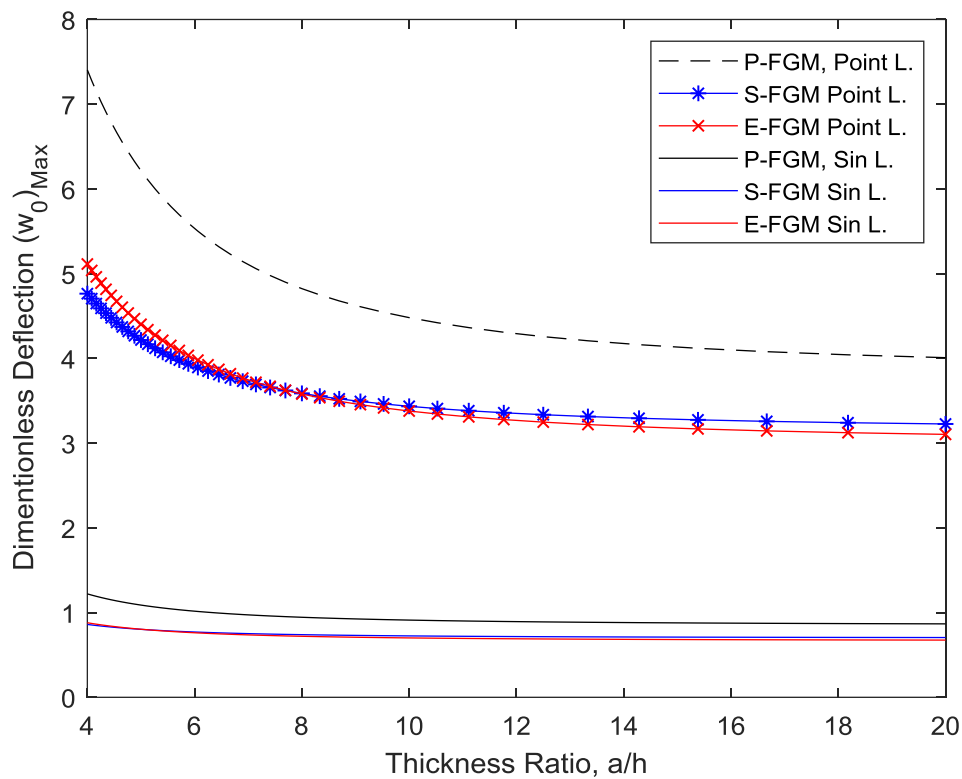


**Figure 17: Differences between classes of FGM plates in terms of the maximum deflection vs. thickness ratios when subjected to a point load and a sinusoidal distributed load**

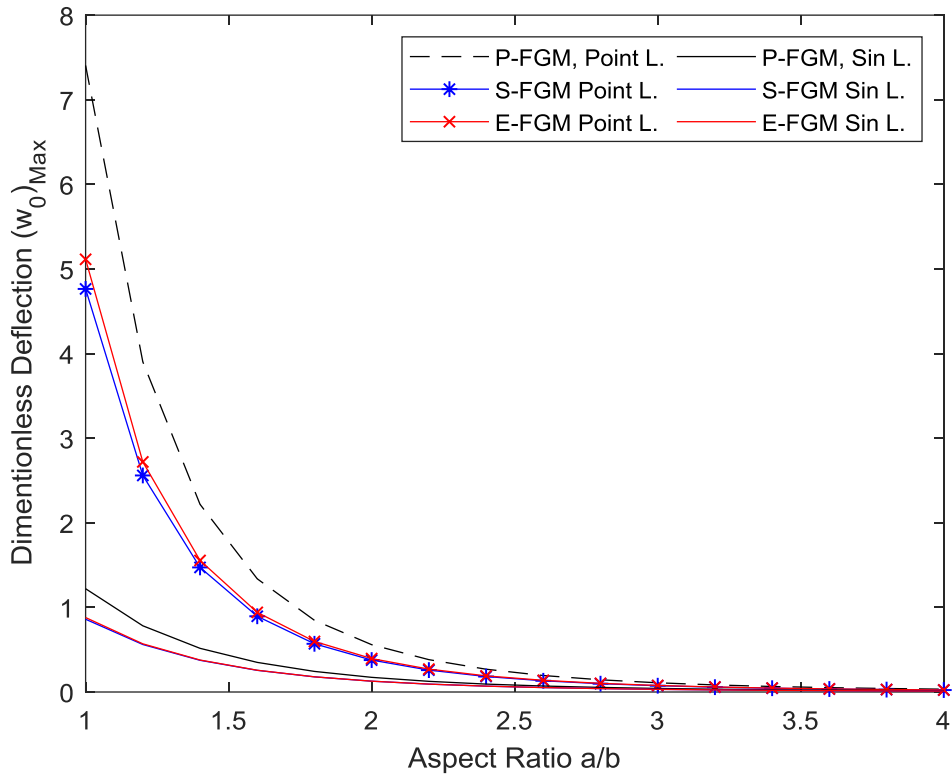


Figure 18: Differences between classes of FGM plates in terms of the maximum deflection vs. aspect ratios when subjected to a point load and a sinusoidal distributed load

#### 4.2.2 Dynamic Responses of Classes of FGM

Dynamic responses of a functionally graded metal-ceramic plate are now under investigation. Unforced vibration behavior of an FGM panel is the actual target of this part, where the fundamental natural frequencies, which means in the Fourier expansion equations (3.77),  $m = n = 1$ , of each type of the volume gradient is investigated. For doing so, the panel is either considered to be in a square shape, with a unity squared meter and simply supported on all sides, or it is considered to have variable side length. Two sorts of examinations are taken to consideration, which are effects of changing ingredient's concentrations across the panel's depth, and how various combinations of ceramic-metal

panels with functionally gradient thickness wise properties would affect the natural frequencies of that panel.

#### **4.2.2.1 Effects of Varying Material Gradient (Power Indices)**

Figure 19 and 20 show the relations between varying the power index and the mode fundamental resonance frequency of an FG composite panel made of aluminum-alumina, for both cases of either variable  $a/h$  or variable  $a/b$  values, respectively. When power indices vary for power and sigmoid distribution functions, Figure 19 and 20 suggest that in either case of low or high-power indices, sigmoid law has higher fundamental frequencies, due to the special features regarding smooth distribution of material properties that the law has, as mentioned before. It can be seen that the effect of increasing the power index, in general, would lower the natural frequency. In addition, the relation between the effect of varying  $a/h$  and the effect of varying  $a/b$ , can somehow be thought as inversely proportional. To be more specific, the higher the values of thickness ratios with a fixed aspect ratio, the smaller the differences between the calculated non-dimensional fundamental frequencies, associated to different gradient functions for various material concentration, are. However, this is completely opposite for the case of variable  $a/b$  values in a thick panel, where increasing make larger differences in the beginning, and then those differences become almost constant.

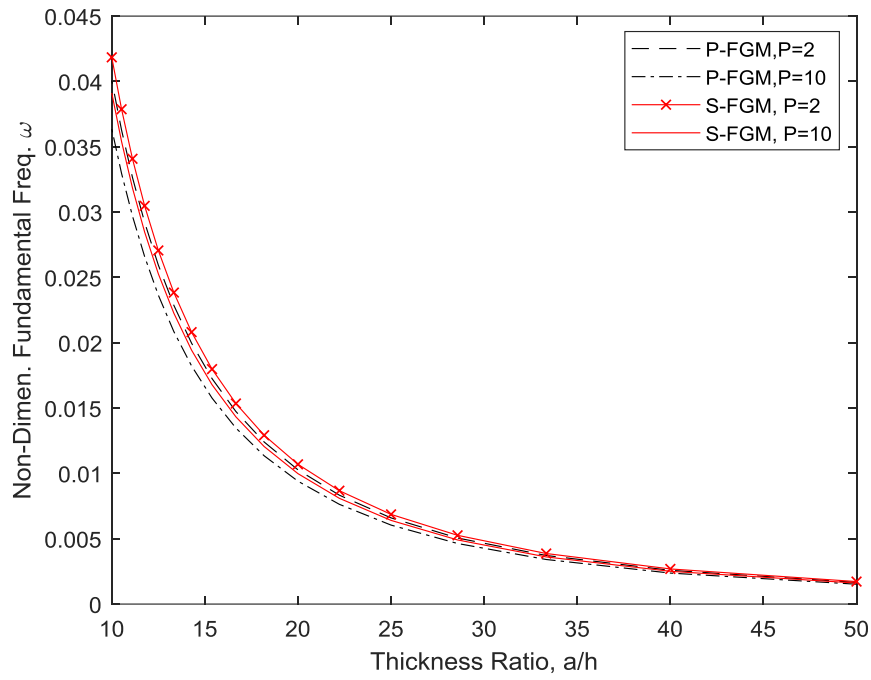


**Figure 19: Effects of varying power indices and thickness ratios on plate's non-dimensional fundamental frequencies of the first mode on P-FGM and S-FGM**

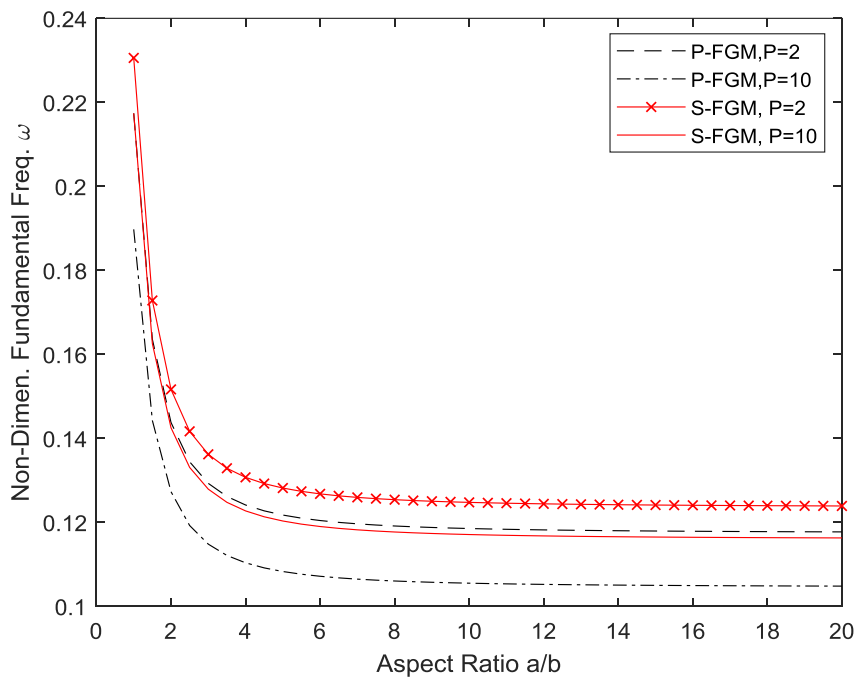


**Figure 20: Effects of varying power indices and aspect ratios on plate's non-dimensional fundamental frequencies of the first mode on P-FGM and S-FGM**

#### 4.2.2.2 Effects of Varying Plate's Constituents

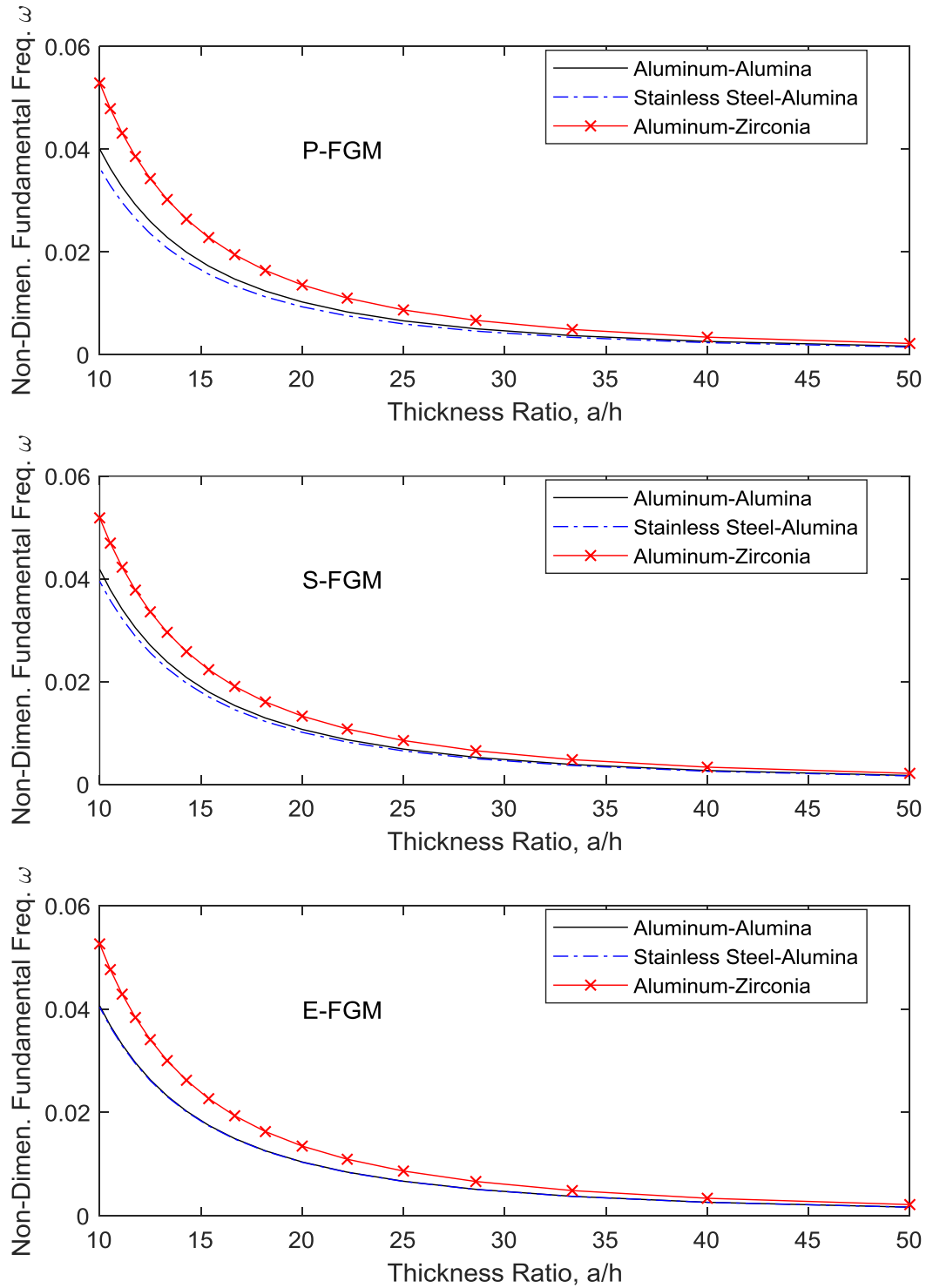
Now for discovering how elastic moduli and mass densities effects the dynamic behavior of an FGM panel, another class of a parametric investigation is conducted for observing the effect of bottom-to-top surfaces properties ratios. In this time, different couples of ceramic-metal combinations are investigated for P-, S- and E-, where the power index equals to 2 for power and sigmoid cases. The material properties of the constituents and properties ratios are shown in Table 5. Then, plates made of a certain couple and manufactured with a specific volume gradient law are investigated along with variable aspect ratios or variable thickness ratios to show how properties' ratios affects the dynamic responses.

**Table 5: Material properties of several combinations of the constituents of a ceramic-metal FGM panels**

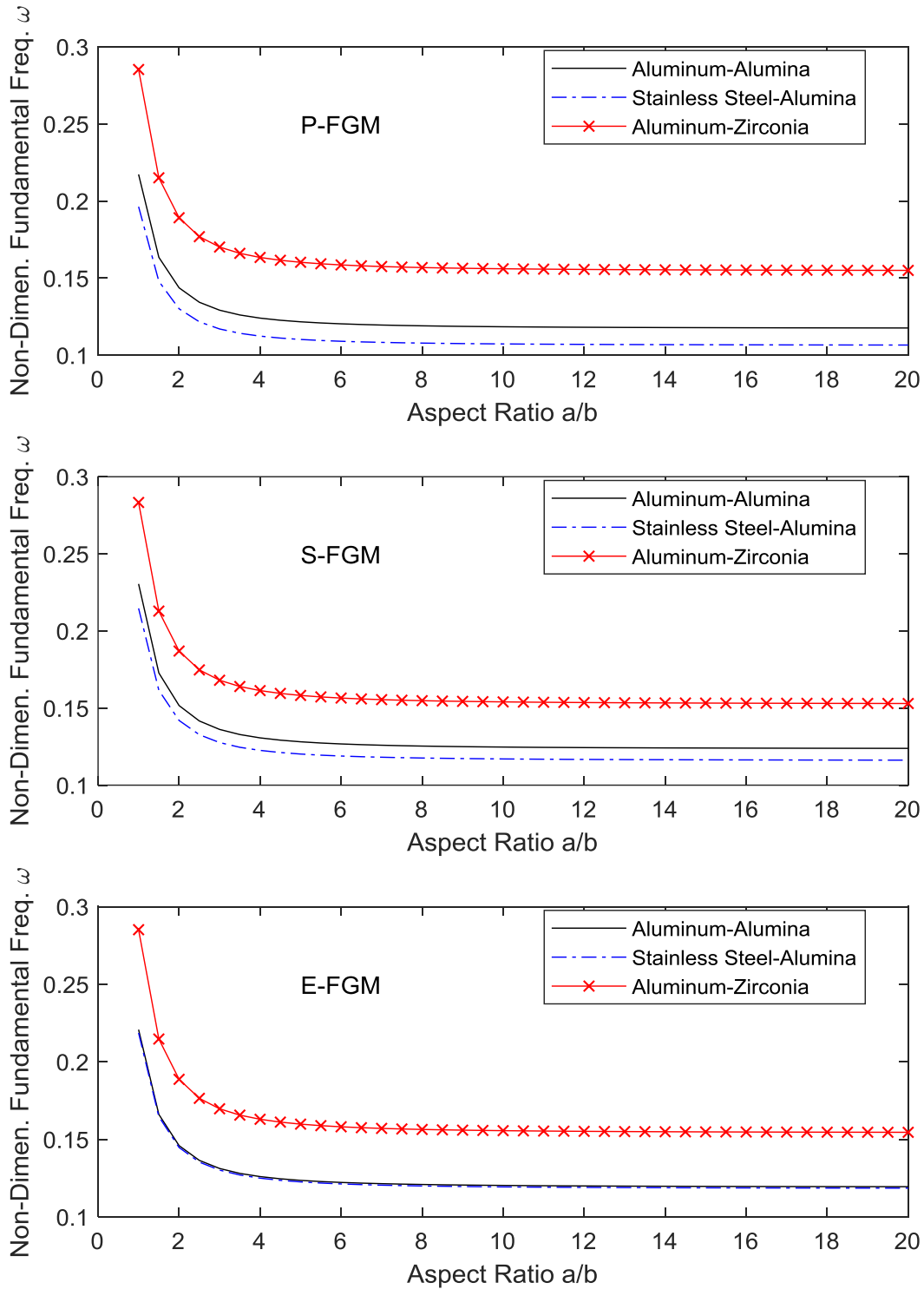
Constituents Combinations	Bottom Surface (Ceramic)		Bottom Surface (Metal)		Properties Ratios	
	$E_1$ (GPa)	$\rho_1$ ( $kg/m^3$ )	$E_2$ (GPa)	$\rho_2$ ( $kg/m^3$ )	$\frac{E_1}{E_2}$	$\frac{\rho_1}{\rho_2}$
Aluminum-Alumina	380	3800	70	2707	5.43	1.4
Stainless Steel- Alumina	380	3800	207	8166	1.84	0.5
Aluminum-Zirconia	200	5700	70	2707	3	2.1

Figure 21 and 22 illustrate the effects of changing an FG plate's ingredients, which necessarily means that changing young's modulus ratios and density ratios for a square variable-thickness panel and a rectangular variable-side-length thick panel, respectively. For dynamic responses, ductility is not the only factor that affect the panels behavior, but the mass density would have a strong effect too. In fact, the effect of  $E_1/E_2$  ratio is less in the dynamic stage compared to the static one. According to Figure 21 and 22, Aluminum-Zirconia combination has the highest natural frequency for all types of FGM, although it does not have the highest elastic ratio, but it has in fact the greatest ceramic-to-metal density ratio, which confirm the conclusion made earlier regarding high influence of density ratios on the dynamic responding. Nest, the combinations made of stainless steel-alumina and aluminum-alumina show lower natural frequencies, in general, and they exhibit minimum frequency for the case of E-FGM.

However, these differences start to vanish when the square panel becomes thinner, since the volume fraction through the thickness has less significance. On the other hand, for a rectangular with variable a/b ratios FG thick panel, the influence elongating the plate would first increase the differences between the natural frequencies to a certain limit (almost for a/b greater than 4), where then those differences remain the same.



**Figure 21: Effects of varying surfaces constituents and thickness ratios on the plate's fundamental frequencies of the first mode for a) P-FGM, b) S-FGM and c) E-FGM, from top to bottom plots, respectively.**



**Figure 22: Effects of varying surfaces constituents and aspect ratios on the plate's fundamental frequencies of the first mode for a) P-FGM, b) S-FGM and c) E-FGM, from top to bottom plots, respectively.**



Overall, the following general observations are made during the previous study. First, the conducted parametric study proves that, varying the power indices and the material stiffnesses would have a greater impact on the static response of any type of functionally gradient panel. Second, when compared to each other, power law distribution would always have higher deflection (except when  $p$  is less than 1) and lower fundamental frequencies compared to others, due to the sudden and rapid change in the material properties closer to the interface. Third, the effect of elongating a thick FGM plate, in terms of the statics, would make it behave more likely as a beam, that is decreasing the maximum deflection and vanishing all the effects of varying all other factors, such as varying volume fraction laws, power indices, elastic moduli ratios or even changing the type of the applied force. Moreover, for dynamic cases, increasing aspect ratios lead to lowering the plate's natural frequencies with dramatic rates in the beginning up to a specific limit, where a further increase in the plate's length would be redundant with respect to lower plate's natural frequency. Finally, varying  $a/h$  ratios, i.e. thinner square panels, have lower rates of influences, on both static and dynamic perspectives, compared to the rate of influence that the  $a/b$  ratios have.

## CHAPTER 5

### EFFECTS OF SHEAR DEFORMATION

Materials that have gradient properties across a direction, i.e. functionally graded materials, are most likely to be utilized in rectangular panels structures. Therefore, one of interesting and considerable nature of panels is shear deformations. This terminology refers to the distortion inside a panel that takes place when a plate is subjected to a transverse external force, so that a normal transverse line would no longer be perpendicular to the mid-surface.

When transverse pressures or forces are applied on an FGM panel, a shear deformation occurs across the thickness. However, the necessity encountering the influence of that deformity in the procedures of predicting mechanical behaviors of an FG panel may vary from as low as trivial to as high as significant effectiveness. The key point of determining whether to include the shear deformation or not, is truly about how long is the normal distance between the top interface to the lower interface of a rectangular panel compared to its length (or width), in other words, a panel's thickness compared to its aspect ratio is the major player. To investigate the role of an FG plate's thickness, an FGM plate's behavior, which has variable thickness ratios, is under consideration, with two most commonly used panel's theories.

The theories, which are under investigation, are the theory of small deflections of plates, or better known in the FG literatures as the classical plate theory (CPT), and the theory of third order shear deformation, (TSDT). The first theory is the simplest form for

describing the displacement field of an FGM panel, and the assumptions which the theory is based on are mentioned in the Mathematical Formulation of FGM Panels chapter. However, the simplicity of CPT imposes it to sacrifice the accuracy, specially for thicker panels, since, unlike TSDT, which accounts for the effect of shear deformation, CPT, by its assumptions, does not take care of this effect.

## 5.1 Shear Effects on Maximum Deflection

Observing how deformation related to transverse shear affects an FG panel's static response, namely the panel's maximum deflection, could be done by comparing the results obtained predicting the maximum deflection using CPT and TSDT, for various side-to-thickness ratio of a square plate, and various aspect ratios for thick plates. To do so, a simply supported plate with functionally graded ingredients undergoing a uniformly distributed pressure of  $100 \text{ kN/m}^2$  manufactured with 3 different techniques, i.e. power, sigmoid and exponential functions, is studied. Moreover, for the case of variable thickness ratios corresponding to a constant aspect ratio, consider a square plate that has an area of 1 squared meter, and it is made of ceramic-metal combination constituents, namely aluminum alumina, whose properties are already listed in Table 2. Moreover, for showing the effects of aspect ratios, a rectangular FG plate with a fixed thickness ratio (a thick panel) is considered.

To illustrate the effects of including shear defamation, as compared to earlier models of CPT for the cases of thick FG plates, Figures 23 and 24 show results of calculating the expected maximum deflection obtained by CPT and TSDT of the three functions representing different cases of material volume coefficient distribution. In these figures,

the result is defined as the percentage increase in predicted displacement calculated using HSDT over the results calculated using CPT.

Figure 23 and 24 shows the general tendency of TSDT to deviate from CPT expectation of FGM panels maximum deflection when the side length-to-thickness ratio shrinks, i.e. the plate becomes thicker, and for lower aspect ratios ( $a/b < 2$ ). This results perfectly align with what just stated before regarding the magnification of shear effects when the plate thickness adds up and the aspect ratio decreases. Therefore, the aspect ratio has a similar effect with the thickness ratio, since increasing both of them relief the shear deformation effects. Moreover, the figures also confirm the earlier conclusion about the overall superiority of P-FGM deflections compared to the others, because of the steep gradient of material properties near the interface.

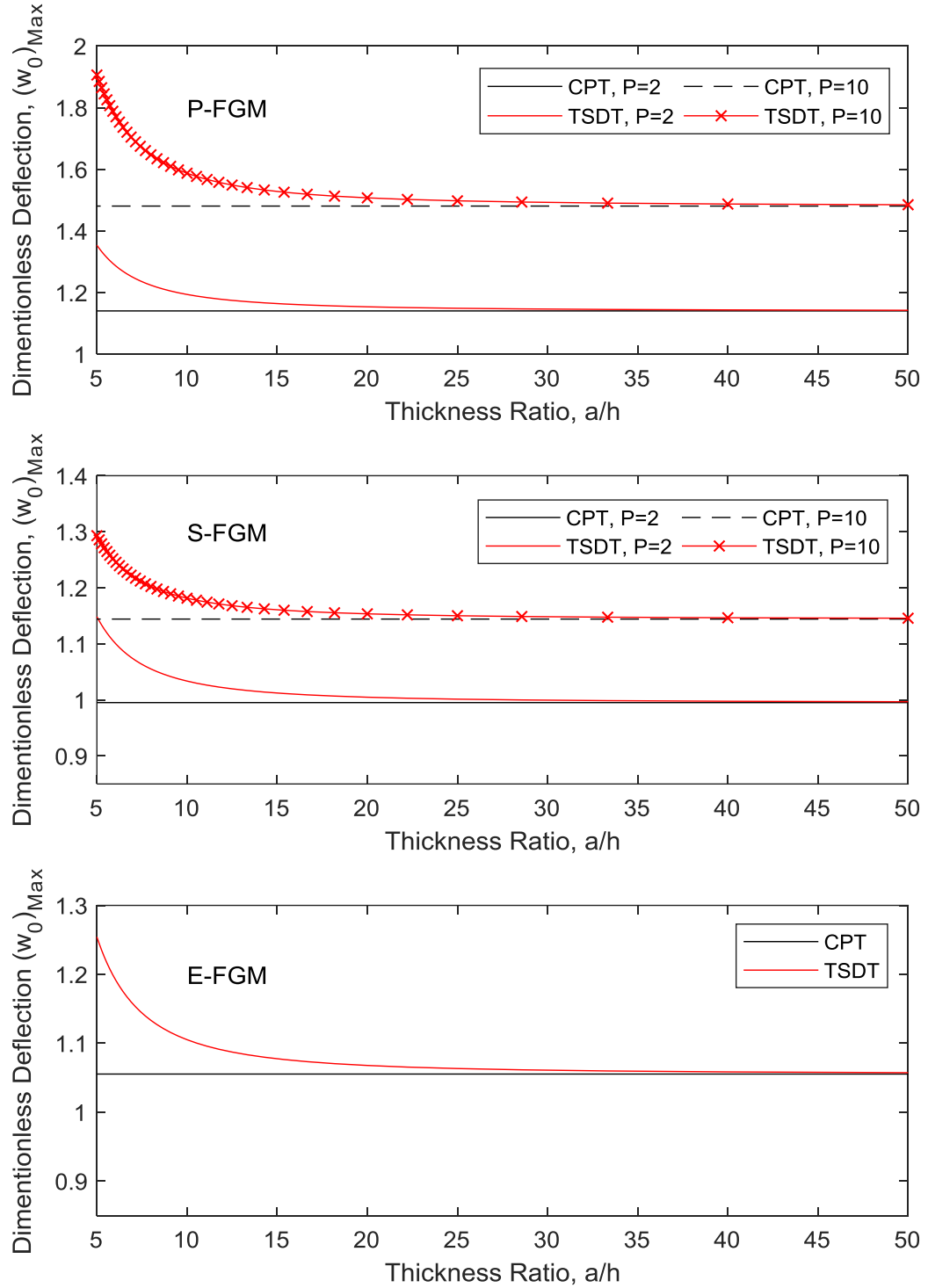
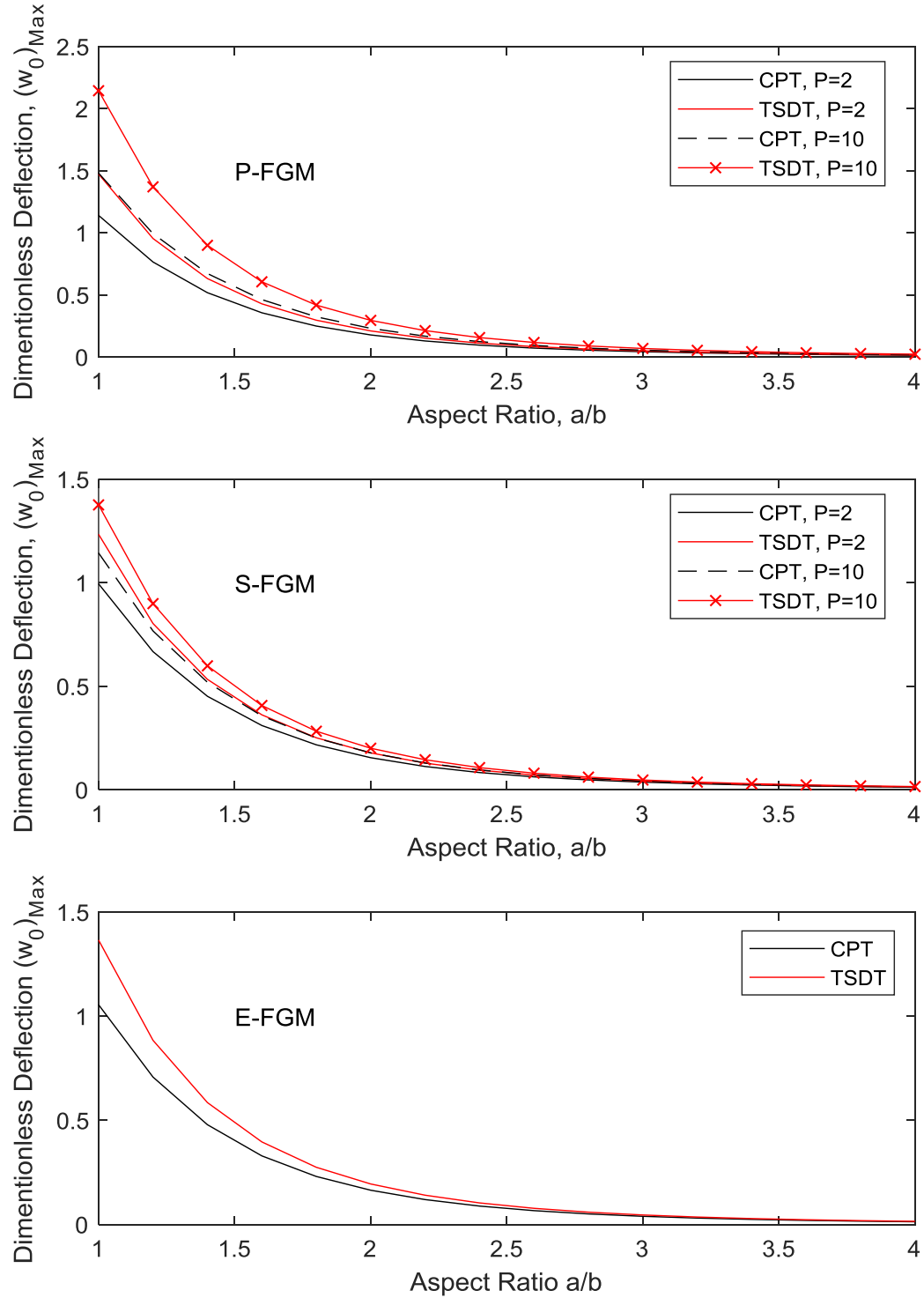


Figure 23: Effect of Shear deformation in terms of various thickness ratios on predicting the dimensionless deflections of a) P-FGM, b) S-FGM and c) E-FGM, from top to bottom plots, respectively.



**Figure 24: Effect of Shear deformation in terms of various aspect ratios on predicting the dimensionless deflections of a) P-FGM, b) S-FGM and c) E-FGM, from top to bottom plots, respectively.**

To obtain more details of how significantly the shear deformation effects can influence the prediction of a plate's static response, tables 6 and 7 describe the dimensionless deflections for certain thickness ratios with increasing power indices for the case of power and sigmoid functionally gradient materials. Observation of tables 6 and 7 confirm that for lower  $a/h$  ratios, or thicker panels, the difference between not including and including the deformation influence can go nearly as high as 30 %, as in the case of P-FGM with a power index equals to 20 and thickness 20 centimeters. However, for thinner panels, the shear effect becomes smaller, and can be neglected. Moreover, Table 6 demonstrates an interesting difference between the nature of power and sigmoid laws when they are implemented for a certain thickness ratio with various power indices. To better describe this difference, Figure 25 is presented next.

**Table 6: Dimensionless Maximum Deflections of P-FGM and S-FGM square plates with various power indices and thickness ratios obtained by CPT and TSDT**

a/h	Power index	P-FGM			S-FGM		
		CPT	TSDT	% Diff.	CPT	TSDT	% Diff.
5	2	1.1406	1.3538	18.7006	0.9952	1.1485	15.4023
	10	1.4807	1.9059	28.7189	1.1442	1.2929	12.9988
	20	1.6763	2.1329	27.2338	1.1577	1.3059	12.7992
10	2	1.1406	1.1940	4.6824	0.9952	1.0336	3.8557
	10	1.4807	1.5872	7.1939	1.1442	1.1814	3.2538
	20	1.6763	1.7907	6.8213	1.1577	1.1948	3.2037
25	2	1.1406	1.1491	0.7495	0.9952	1.0013	0.6171
	10	1.4807	1.4977	1.1516	1.1442	1.1502	0.5208
	20	1.6763	1.6946	1.0920	1.1577	1.1636	0.5128
50	2	1.1406	1.1427	0.1874	0.9952	0.9967	0.1543
	10	1.4807	1.4849	0.2879	1.1442	1.1457	0.1302
	20	1.6763	1.6809	0.2730	1.1577	1.1592	0.1282



**Table 7: Dimensionless Maximum Deflections of E-FGM square plates with various power indices and thickness ratios obtained by CPT and TSDT**

a/h	E-FGM		
	CPT	TSDT	% Diff.
5	1.0553	1.2543	18.8572
10	1.0553	1.1051	4.71904
25	1.0553	1.0633	0.75808
50	1.0553	1.0573	0.18952

As noted from Figure 25, power and sigmoid cases of volume coefficient distribution have different reactions towards changing the intensity index. First, it is clear that in case of power law, the error resulted when predicting the maximum deflection by CPT is significantly higher than sigmoid. For example, when the power index equals 10 for a thickness ratio equals to 5, percentage difference between CPT and TSDT for power FG is more than 15 % higher than sigmoid. Therefore, in general it would be better to completely avoid CPT when dealing with power laws for moderately thick plates. Moreover, it is noticed from the mentioned figure, how percentage difference behaves for each FG type. For power functionally materials panels, the difference between CPT and TSDT magnifies, in a rate that is directly proportional to the plate's thickness, from lower values of P, until it reaches a peak point (around P=10), when the difference starts to settle down gradually to end up with a nearly constant percentage difference. This behavior is totally different

when it comes to sigmoid functions, where the difference will drop first, again with a rate that directly proportional to the plate's thickness. We can also see that, beyond a certain value of a power index, about  $15 < P < 20$ , the difference reaches its lowest value and remains almost constant. It can be inferred that, for moderate to thin S-FGM panels with high values of power indices, the classical theory might be a simple and sufficient tool to initially predict the static response of these panels.

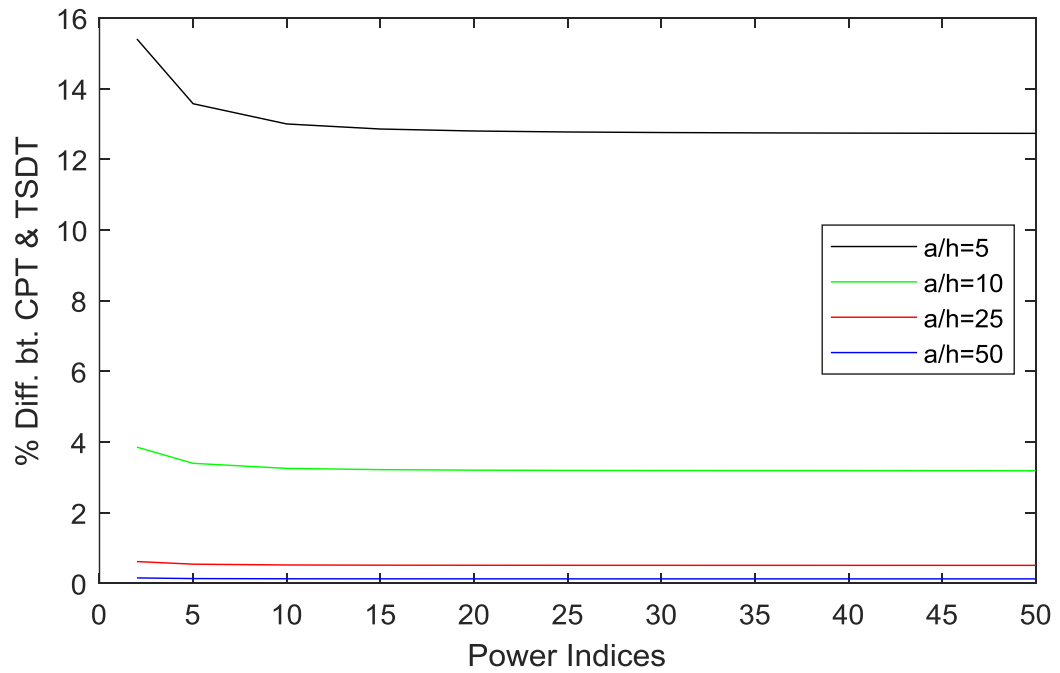
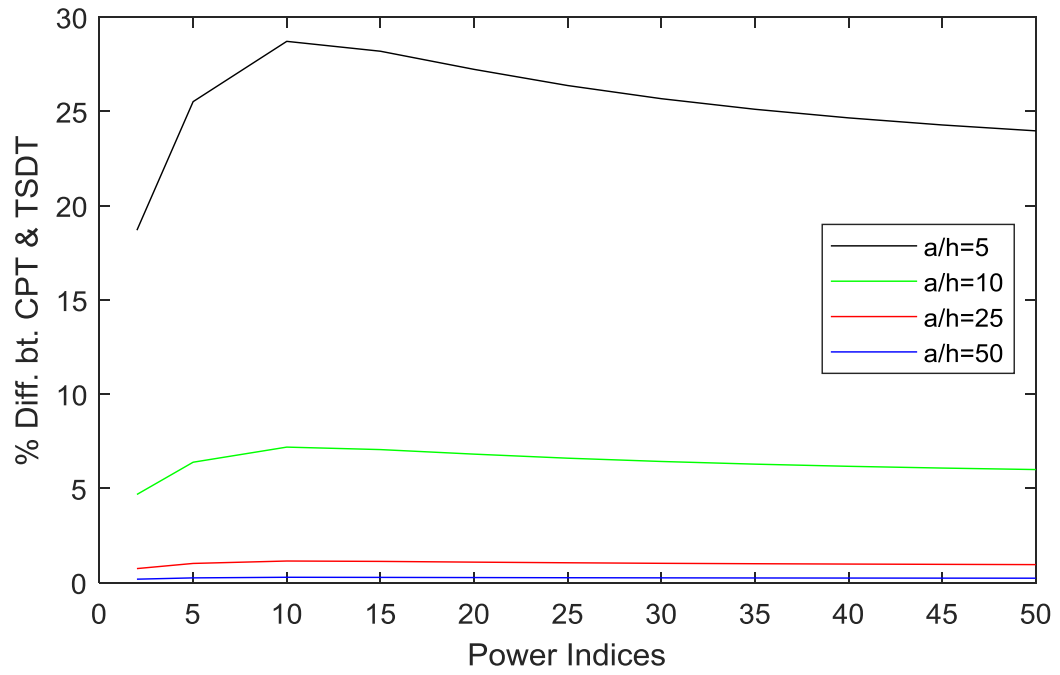


**Figure 25: Effect of power index variation on the percentage increase in maximum deflection calculated using HSDT over CPT results at different aspect ratios for: (a) P-FGM and (b) S-FGM, from top to bottom, respectively.**

Eventually, from the previous discussions, one can conclude that the shear effects can be neglected, therefore utilize the simplest plate theory CPT, for predicting static response of only some classes of FGM panels, for the thin plates, or plates with high aspect ratios. However, for aspect ratios lower than 2, and thickness ratios lower than 20, it is not preferable to rely on CPT for determining the expected deflections, because of the high error in the prediction that occur below those ratios when CPT is utilized.

## **5.2 Shear Effects on Fundamental Natural Frequency**

In order to examine the trace of shear deformation on FGM panels' dynamic behavior. The non-dimensional fundamental natural frequency of power gradient panels is studied for several modes. The panel is assumed to be simply supported and made of aluminum alumina. Results of CPT calculation are gathered from reference [28].

Table 8 illustrates potential errors that might take place when the deflection associated with transverse shear is ignored in the calculations of a power gradient plate that has simple supports on all of its edges. It can be seen that, the deference, in general, is less significant for the case of free vibration compared to static load case. However, a higher error exists in the first mode.

**Table 8: Effect of Shear deformation on the non-dimensional fundamental frequencies refer to the first three modes of P-FGM**

Mode	Power Index	Non-dimensional fundamental Frequency ( $\tilde{\omega}$ )		
		CPT [28]	TSDT	% Difference
1	1	1.4285	1.3967	2.2
	5	1.2299	1.1909	3.2
	10	1.1917	1.1497	3.5
2	1	7.2459	7.2374	0.1
	5	5.6543	5.6399	0.3
	10	5.1537	5.1482	0.1
3	1	12.256	12.2139	0.3
	5	9.5732	9.4976	0.8
	10	8.7209	8.6841	0.4

Eventually, it can be deduced that, in both cases of statics and dynamics, the inclusion of shear deformation effect would have a softening effect on the behavior of thick FG panels. For instance, in the case of maximum deflection, the use of TSDT, which accounts for the effect of shear deformations, showed higher values of maximum deflection compared to CPT. Similarly, the implementation of TSDT leads to predictions of lower values of the fundamental natural frequencies, which is more accurate prediction than CPT.

## CHAPTER 6

### CONCLUSIONS

#### 6.1 Summary

This work started by reviewing the basic concepts and applications of laminated and functionally graded composite materials. A comprehensive detailed literature review of recent development of modeling the response of thin, moderately thick, and thin FGM plates. As a result, some research gaps were identified, and the thesis objective was formulated as the development of a model capable of calculating deformations and natural frequencies of thick P-, S-, and E-FGM panels. After reviewing available plate theories, the mathematical modeling of the stated problem was developed, in chapter 4, using TSDT. Navier-type expansions were used to solve for the unknown expansion coefficients.

Results of the MATLAB codes were verified using comparisons with available P-FGM published results for the static and dynamic cases. A parametric study on all types of FGM plates was conducted, and the effect of shear deformations on the calculations accuracy was evaluated. The results of this study can be summarized in the following:

1. The maximum deflection increases with the power index in both P-FGM and S-FGM plates due to the decreased plate stiffness.
2. For power indices higher than 1, P-FGM exhibits more deflection compared to S-, indicating decreased stiffness, and the opposite occurs for cases with power index less than 1.

3. The increase in the thickness ratio  $a/h$  tends to have smaller influence compared to an increase in the aspect ratio (for  $a/b > 4$ ) for varying the power indices or elastic ratios, because the length of the plate becomes the dominating factor affecting deflection.
4. The effect of parametrizing  $E_1/E_2$  ratio alone on FGM plates static behavior is that, increasing  $E_1/E_2$  magnifies the differences between the deflections of each volume fraction, with the lowest deflection associated with S-FGM, then E-FGM, while P-FGM has deflection due to its nature of sudden change in material properties closer to the interfaces. Moreover, the closer the elastic ratios to one, the smaller the difference in maximum deflections between the three classes.
5. The observed behavior is the same for different types of transverse loading in the static case, in general.
6. Varying power indices for P- and S-FGM has smaller impact on natural frequencies than on static deflections.
7. Increasing plate aspect ratio reduces the fundamental frequency at a decreasing rate, that changes with the type of the plate material function.
8. As thickness ratio decreases, indicating thinner FGM panels, the effect of material distribution function on the fundamental frequency becomes less significant.
9. Including transverse shear deformation shows similar effects on P-, S-, and E-FGM plates at all values of thickness ratio.

10. The influence of neglecting the shear effects for thick FG panels, i.e. using CPT for the prediction static and dynamic behaviors of the panels, leads to hardening effects (predicting lower deflections, and higher natural frequencies.)

## **6.2. Aspects for Improvements in Future Work**

The following areas can be considered as potential aspects for future work:

1. Mechanical behaviors of thick S- and E-FGM plates under different support conditions.
2. Transient forced response of thick S- and E- FGM plates.
3. Integration of the developed model with a FEM solver and an optimization algorithm to provide an easy to use design tool for thick FGM structures.
4. Utilization of genetic algorithms in order to study plate response under material uncertainties
5. Extending the work to cover sandwich structures with S-FGM plate covers, which have the advantage of reduced interface mismatch of properties.



## References

- [1] Udupa, G., Rao, S. S., & Gangadharan, K. (2014). Functionally Graded Composite Materials: An Overview. *Procedia Materials Science*, 1292-1299.
- [2] Chi, S., & Chung, Y. (2006). Mechanical behavior of functionally graded material plates under transverse load—Part I: Analysis. *International Journal of Solids and Structures*, 43(13), 3657-3674. doi:10.1016/j.ijsolstr.2005.04.011
- [3] Swaminathan, K., Naveenkumar, D., Zenkour, A., & Carrera, E. (2015). Stress, Vibration and Buckling Analyses of FGM Plates—A State of The Art Review. *Composite Structures* , 11-26.
- [4] Reddy, J. N., & Cheng, Z. (2001). Three-Dimensional Solutions of Smart Functionally Graded Plates. *Journal of Applied Mechanics*, 68, 234-241.
- [5] Vel, S. S., & Batra, R. (2004). The three-dimensional exact solution for the vibration of functionally graded rectangular plates. *Journal of Sound and Vibration*, 272(3-5), 703-730. doi:10.1016/s0022-460x(03)00412-7
- [6] Zenkour, A. M. (2006). Generalized shear deformation theory for bending analysis of functionally graded plates. *Applied Mathematical Modelling*, 30(1), 67-84. doi:10.1016/j.apm.2005.03.009
- [7] Peng, X.L. and Li, X.F., “Thermoelastic analysis of functionally graded annulus with arbitrary gradient,” *Appl Math Mech*, Vol. 30, No. 10, pp. 1211-1220, 2009.

- [8] Şimşek, M. (2010). Fundamental frequency analysis of functionally graded beams by using different higher-order beam theories. *Nuclear Engineering and Design*, 240(4), 697-705.
- [9] Tornabene, F., Fantuzzi, N., & Baccocchi, M. (2014). Free vibrations of free-form doubly-curved shells made of functionally graded materials using higher-order equivalent single layer theories. *Composites Part B: Engineering*, 67, 490-509.
- [10] Javaheri, R., & Eslami, M. R. (2002). Thermal Buckling of Functionally Graded Plates. *AIAA Journal*, 40, 162-169.
- [11] Chi, S., & Chung, Y. (2006). Mechanical behavior of functionally graded material plates under transverse load —Part II: Numerical results. *International Journal of Solids and Structures*, 3675-3691.
- [12] Ashrafi, H. R., Beiranvand, P., Aghaei, M. Z., & Jalili, D. D. (2018). Modal Analysis of FGM Plates (Sus304/Al<sub>2</sub>O<sub>3</sub>) Using FEM. *Bioceram Dev Appl*, 8(112), 2.
- [13] Zhao, X., Lee, Y. Y., & Liew, K. M. (2009). Free vibration analysis of functionally graded plates using the element-free kp-Ritz method. *Journal of sound and Vibration*, 319(3-5), 918-939
- [14] Hosseini-Hashemi, S., Taher, H. R. D., Akhavan, H., & Omid, M. (2010). Free vibration of functionally graded rectangular plates using first-order

- shear deformation plate theory. *Applied Mathematical Modelling*, 34(5), 1276-1291
- [15] Thai, H. T., & Choi, D. H. (2013). A simple first-order shear deformation theory for the bending and free vibration analysis of functionally graded plates. *Composite Structures*, 101, 332-340
- [16] Bellifa, H., Benrahou, K. H., Hadji, L., Houari, M. S. A., & Tounsi, A. (2016). Bending and free vibration analysis of functionally graded plates using a simple shear deformation theory and the concept the neutral surface position. *Journal of the Brazilian Society of Mechanical Sciences and Engineering*, 38(1), 265-275.
- [17] Reddy, J. N. (2000). Analysis of Functionally Graded Plates. *International Journal for Numerical Methods in Engineering*, 663-684.
- [18] Qian, L., Batra, R., & Chen, L. (2004). Static and dynamic deformations of thick functionally graded elastic plates by using higher-order shear and normal deformable plate theory and meshless local Petrov–Galerkin method. *Composites Part B: Engineering*, 35(6-8), 685-697.  
doi:10.1016/j.compositesb.2004.02.004
- [19] Matsunaga, H. (2008). Free vibration and stability of functionally graded plates according to a 2-D higher-order deformation theory. *Composite structures*, 82(4), 499-512.

- [20] Natarajan, S., & Manickam, G. (2012). Bending and vibration of functionally graded material sandwich plates using an accurate theory. *Finite Elements in Analysis and Design*, 57, 32-42.
- [21] Bessaim, A., Houari, M. S., Tounsi, A., Mahmoud, S. R., & Bedia, E. A. A. (2013). A new higher-order shear and normal deformation theory for the static and free vibration analysis of sandwich plates with functionally graded isotropic face sheets. *Journal of Sandwich Structures & Materials*, 15(6), 671-703.
- [22] Belabed, Z., Houari, M. S. A., Tounsi, A., Mahmoud, S. R., & Bég, O. A. (2014). An efficient and simple higher order shear and normal deformation theory for functionally graded material (FGM) plates. *Composites Part B: Engineering*, 60, 274-283.
- [23] Akbarzadeh, A. H., Zad, S. K., Eslami, M. R., & Sadighi, M. (2010). Mechanical behaviour of functionally graded plates under static and dynamic loading. *Proceedings of the Institution of Mechanical Engineers, Part C: Journal of Mechanical Engineering Science*, 225(2), 326-333.  
doi:10.1243/09544062jmes2111
- [24] Hosseini-Hashemi, S., Fadaee, M., & Atashipour, S. (2011). Study on the free vibration of thick functionally graded rectangular plates according to a new exact closed-form procedure. *Composite Structures*, 93(2), 722-735.  
doi:10.1016/j.compstruct.2010.08.007

- [25] Mantari, J. L., Oktem, A. S., & Soares, C. G. (2012). Bending response of functionally graded plates by using a new higher order shear deformation theory. *Composite Structures*, 94(2), 714-723.
- [26] Mantari, J. L., & Soares, C. G. (2012). Bending analysis of thick exponentially graded plates using a new trigonometric higher order shear deformation theory. *Composite Structures*, 94(6), 1991-2000.
- [27] Mantari, J. L., & Soares, C. G. (2013). A novel higher-order shear deformation theory with stretching effect for functionally graded plates. *Composites Part B: Engineering*, 45(1), 268-281.
- [28] Mechab, I., Mechab, B., & Benaissa, S. (2013). Static and dynamic analysis of functionally graded plates using Four-variable refined plate theory by the new function. *Composites Part B: Engineering*, 45(1), 748-757.  
doi:10.1016/j.compositesb.2012.07.015
- [29] SiddaReddy, B., Kumar, J. S., EswaraReddy, C., & Reddy, K. (2014). Static Bending Behavior of Functionally Graded Plates Subjected to Mechanical Loading. *Jordan Journal of Mechanical & Industrial Engineering*, 8(4).
- [30] Thinh, T. I., Tu, T. M., Quoc, T. H., & Long, N. V. (2016). Vibration and buckling analysis of functionally graded plates using new eight-unknown higher order shear deformation theory. *Latin American Journal of Solids and Structures*, 13(3), 456-477.

- [31] Elishakoff, I., Pentaras, D., & Gentilini, C. (2016). *Mechanics of Functionally Graded Material Structures*. NJ: World Scientific.

## Vitae

Name : Sultan M. Ghazzawi

Nationality : Saudi

Date of Birth : 1/12/1993

Email : sultan.ghazzawi@hotmail.com

Address : P.O. Box # 2304, KFUPM, Dhahran, 31261, Saudi Arabia

Academic Background : MS in Aerospace Engineering, KFUPM, 2018

BS in Applied Aerospace Engineering, KFUPM, 2016

### Publications

1. Ghazzawi, S. and Abdelrahman, W., "Effect of Transverse Shear Deformation on Response of S-FGM Panels," Accepted for presentation in AIAA Science and Technology Forum and Exposition 2019, San Diego, California, 7-11 Jan. 2019.
2. Ghazzawi, Abdelrahman, W.G. "Effect of Shear Deformation on Static Behavior of Functionally Graded Material Panels," presented in 9th KFUPM Student Forum, 2018